MICRODISK FABRICATION BY EMULSION EVAPORATION

A Thesis

by

SUSANNA WING MAN WONG

Submitted to the Office of Graduate Studies of
Texas A&M University
in partial fulfillment of the requirements for the degree of

MASTER OF SCIENCE

May 2006

Major Subject: Chemical Engineering

MICRODISK FABRICATION BY EMULSION EVAPORATION

A Thesis

by

SUSANNA WING MAN WONG

Submitted to the Office of Graduate Studies of
Texas A&M University
in partial fulfillment of the requirements for the degree of

MASTER OF SCIENCE

Approved by:

Chair of Committee,	Zhengdong Cheng
Committee Members,	Michael A. Bevan
	Raymond E. Schaak
Head of Department,	Kenneth R. Hall

May 2006

Major Subject: Chemical Engineering

ABSTRACT

Microdisk Fabrication by Emulsion Evaporation. (May 2006)

Susanna Wing Man Wong, B.S., University of California, San Diego

Chair of Advisory Committee: Dr. Zhengdong Cheng

Colloidal suspensions of disk-like particles have been of interest in both colloidal and liquid crystal studies because they exhibit unique liquid crystalline phases different from those of rod-like molecules. Disk-like particles, such as asphaltenes in heavy oil industry, clay particles in agriculture, and red blood cells in biology, are of great interest in a variety of industries and scientific areas. However, to fabricate monodisperse microdisks, uniform in structure or composition with precise control of particle size and shape has not yet succeeded. In this thesis, we show an experimental strategy of using microfluidic technique to fabricate homogeneous α-eicosene microemulsions with chloroform in an aqueous solution of sodium dedecyl sulfate (SDS). The monodisperse chloroform emulsions, generated by the glass-based microfluidic devices, ensure the precise control on microdisk particle size and shape. A systematic investigation was performed to study the relation between the resulted microdisk size and the initial concentration of α-eicosene in chloroform before evaporation. The smectic liquid crystalline phase inside the wax particles controls the coin-like disk shape below the melting temperature of wax's rotator phase. The kinetics of the disk formation is observed using a polarized light microscope. Dynamic light scattering is used to characterize the Brownian motion of the microdisks, and the rotational diffusion is estimated from the image sequences taken by the charge-coupled device (CCD) camera.

Effort has been put into collecting a large quantity of microdisks to investigate the discotic liquid crystalline phases, which can be readily probed by light scattering and microscope. In comparison, X-ray and neutron have to be used for the atomic liquid crystalline phase investigation.

To my grandmother, my parents and my sisters

ACKNOWLEDGEMENTS

I would like to thank my committee chair, Dr. Zhengdong Cheng, and my committee members, Dr. Michael A. Bevan and Dr. Raymond E. Schaak, for their guidance and support throughout the course of this research.

Thanks also to my colleagues, the department faculty and staff for making my time at Texas A&M University a great experience.

Finally, thanks to my parents and my sisters for their love and support.

TABLE OF CONTENTS

LIST OF FIGURES

FIGURE Pages

FIGURE Pages

FIGURE Pages

CHAPTER I

INTRODUCTION

Liquid Crystals

Liquid crystals were first discovered in 1888 by the Austrian chemist Friedrich Reinitzer when he was conducting experiments on a cholesterol based substance. He discovered that the substance has two different melting points, and later on, he named this material as “liquid crystal” since it shares both properties of solid and liquid phase.

Between liquid and solid phases, liquid crystals appear in different phases when temperature changes. Isotropic phase is the one that has the property closest to liquid phase. It has the highest number of symmetry and lowest ordering of molecules because the molecules are all randomly aligned into different directions. Figure 1.1 shows different phases of liquid crystals of rod like molecules. When temperature is lowered, kinetic energy of molecules in isotropic phase is reduced; molecules in isotropic phase orient themselves into a certain position to maximize entropy and change into nematic phase. Nematic phase has lower symmetry and higher degree of ordering of molecules than the isotropic phase. Molecules in the nematic phase are oriented on average along a particular direction, but they still have random translational motions.

This thesis follows the style of the *AIChE Journal*.

As temperature is further decreased, molecules are changed into the smectic phase. The smectic phase has even lower symmetry and higher degree of ordering than the nematic phase. Molecules in the smectic phase are aligned into layers or planes. They have translational motions within a single layer, but not between layers. As temperature is further decreased, the smectic phase will be changed into the crystalline phase. Crystalline phase has the lowest symmetry and highest degree of ordering because molecules are regularly ordered in position and aligned in only one direction.

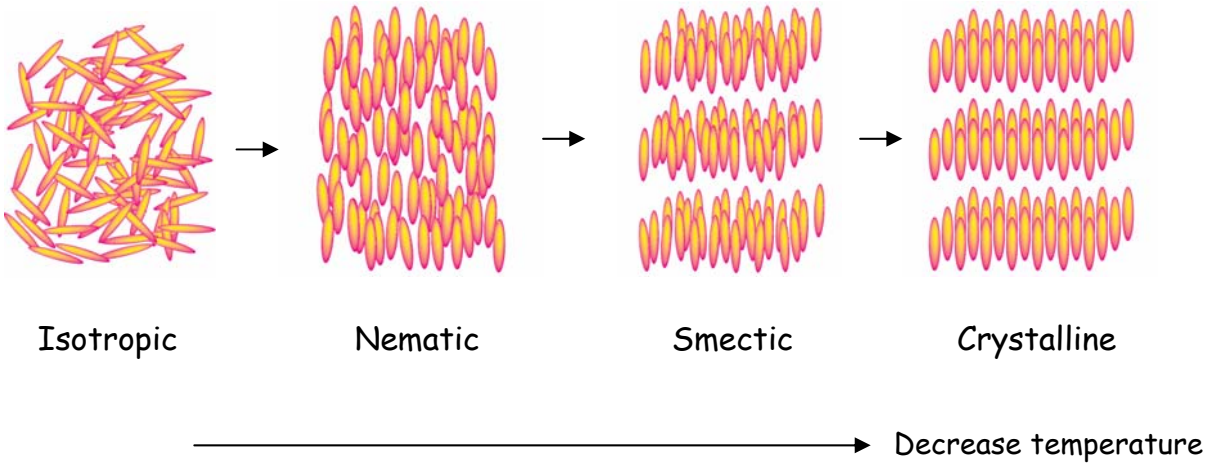

Figure 1.1. Different phases of liquid crystals of rod-like molecules between liquid and solid phase. As temperature decreases, molecules change from isotropic, nematic, smectic, and finally to the crystalline phase.

Liquid crystals made of disk shaped molecules or particles are the least studied compared to others made of, for example, rod shaped molecules or particles. This thesis contributes to the study of discotic liquid crystals by producing uniform wax disks obtained from chloroform solution droplets.

Similarly to the rod shape molecules, disk shaped molecules can also orient themselves into discotic isotropic, discotic nematic, and discotic columnar phases. Figure 1.2 shows different phases of discotic liquid crystals. Depending on the temperature, disk concentration, or pressure, discotic liquid crystals change from isotropic, to nematic, then to columnar phase. For example, by decreasing the temperature, columns in discotic columnar phase will orient themselves into hexagonal or some other rectangular shapes. Research has shown that different tilt angles of disk shaped molecules in columnar phase liquid crystals can form different shapes of columnar phase such as hexagonal, rectangular, oblique, rectangular face-centered, and tilted columns [1].

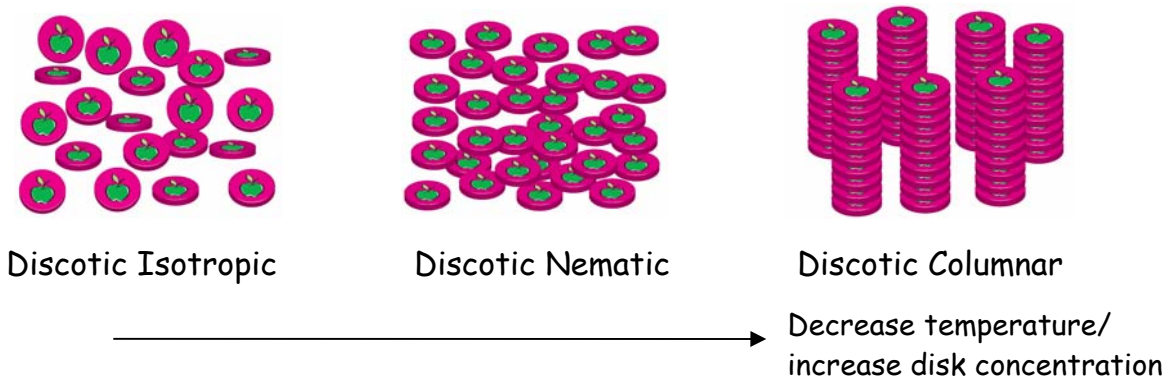

Figure 1.2. Different phases of discotic liquid crystals of disk-like molecules. As temperature decreases or disk concentration increases, discotic liquid crystals change from isotropic, nematic, then to columnar phase.

Emulsions

Emulsion is a mixture of two immiscible liquids. They stay as two separate layers with a boundary between them. One liquid, the dispersed phase, will be dispersed to the other phase, the continuous phase. In our daily life, milk, mayonnaise, and butter are the examples of emulsions. For example, butter has a continuous lipid phase surrounds water droplets, so water-in-oil emulsions are formed. On the other hand, milk is an example of the oil-in-water emulsions.

Emulsions can be unstable because free energy is associated with the interface between the two phases. As more and more emulsions are formed, the interfacial area increases, therefore, more energy is required to keep the emulsions from coalescence. For example, by mixing oil and vinegar salad dressing, unstable emulsions will be formed. In addition, they will aggregate together and small droplets will combine to form larger size droplets if we do not shake it continuously. In order to prevent coalescence, surfactant or emulsifier can be used. For our system, sodium dodecyl sulfate (SDS) is used to serve as a surfactant to stabilize the interface between the two immiscible liquids. Moreover, detergent is another surfactant that will chemically interact with both oil and water, thus stabilizing the interface between oil and water droplets. Besides coalescence, creaming is another property of emulsions. Creaming is the migration of one of the liquids to the top of the emulsion under the influence of buoyancy or gravitational force.

Emulsions are extensively studied by physicists, chemists, and chemical engineers for their novel phase behavior and interfacial properties. Besides emulsions are useful in food industries, they can also be utilized as a template, which is called emulsion template,

to produce porous rutile titanium dioxide [2]. Figure 1.3 demonstrates the monodisperse oil-in-water emulsion droplets that are stabilized by a surfactant and suspended in a second immiscible liquid, titania sol. It is because macroporous titania can undergoes phase transition to rutile phase by calcination without collapse of the pore structure. Monodispersity of emulsions is an important factor that people consider in colloidal science, because a wide size distribution will prevent the crystalline phases formation [3].

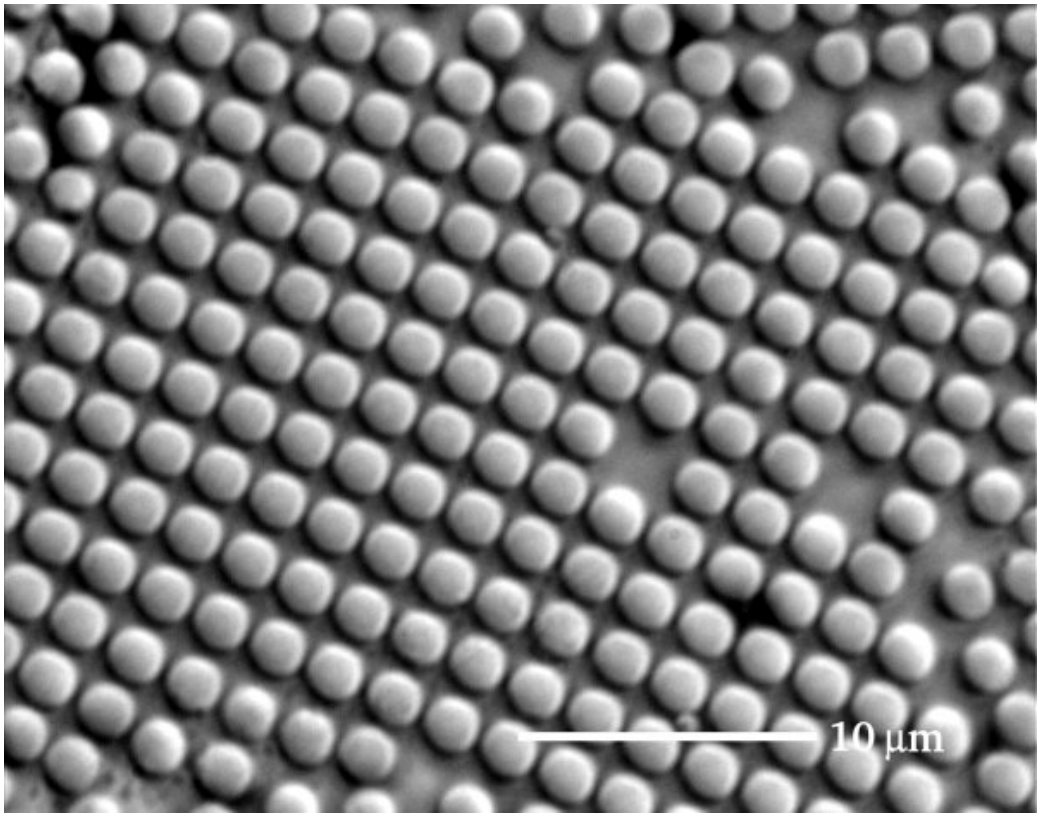

Figure 1.3. Monodisperse oil-in-water emulsions formed an order arrangement [3].

Microfluidics

Microfluidics is a technology in which it handles and deals with small quantities of fluids. The advantages lies in low production cost per device and low power to operate. Also, it occupies small physical space and materials for performing experiments, so reagents and reactants can be used efficiently. Moreover, volume and flow rates can be controlled precisely, and it gives a fast response time.

Flow in microfluidic channels has been studied for years. Reynolds number (Re) can be applied to characterize the channel flow $\mathrm{Re} = l v \rho / \mu$, where l is the dimension of the capillary, v is the velocity of flow, ρ is the density of the fluid, and μ is the viscosity of the fluid [4]. For microfluidic channel flow, Reynolds number is always small, Re < ~2000, so that the flow can be considered as laminar.

In order to fabricate microfluidic devices, different kinds of materials have been utilized successfully in science fields, especially in chemistry and biotechnology. Polydimethylsiloxane (PDMS) is the one widely used today in microfluidics [5-7]. PDMS is a material that is durable and chemically inert, non-toxic, non-flammable and optically transparent. It is intensively used also because it is inexpensive, flexible, and can be molded with high fidelity. Although it is commonly used, PDMS is extremely hydrophobic and has a strong tendency to adsorb other molecules onto the surface [8]. Therefore, in our experiment glass microfluidic device has been fabricated and used successfully to avoid the hydrophobicity problem of PDMS, since α-eicosene involved in

our experiment is hydrophobic. Figure 1.4 demonstrates the fabrication of microfluidic device by using polydimethylsiloxane (PDMS) [9].

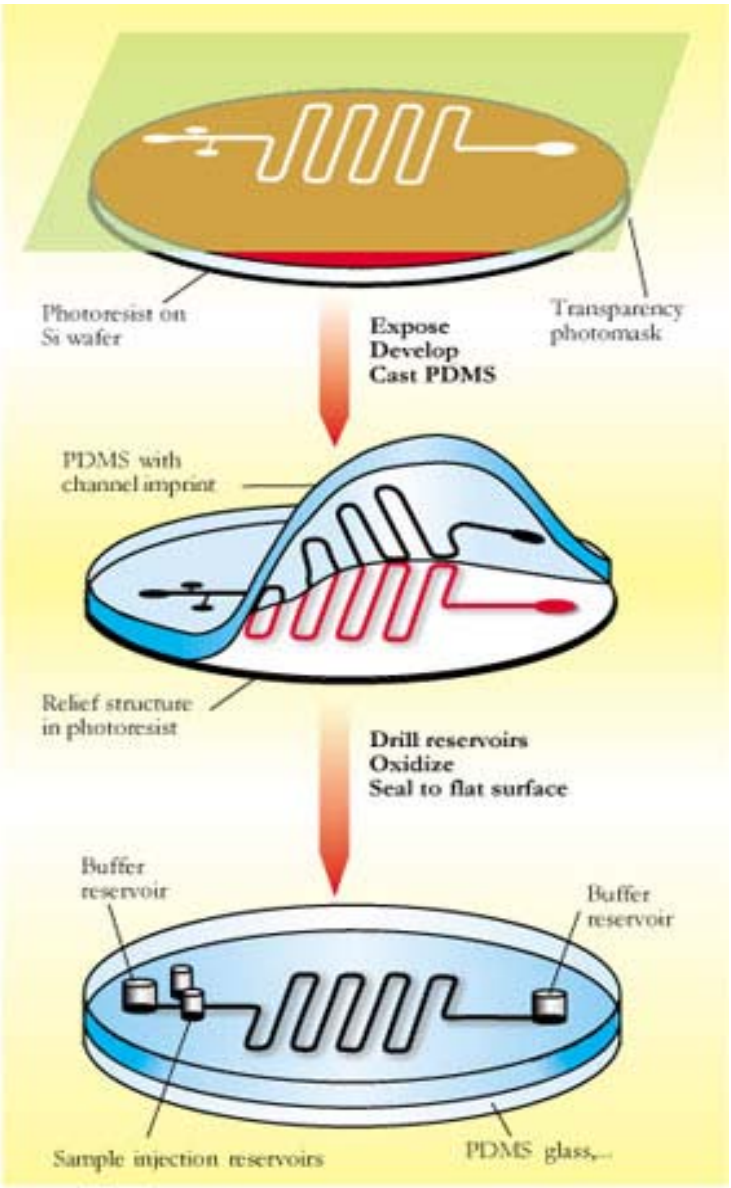

Figure 1.4. Fabrication of microfluidic device by using polydimethylsiloxane (PDMS) [9].

CHAPTER II

COLLOIDAL PARTICLE FORMATION VIA DROPLET EVAPORATION

Emulsion evaporation is used to generate the wax particles. By calculating the final number of wax particles generated during solvent evaporation, we observed that wax solution droplets are split into multiple small wax particles.

Wax Contained Chloroform Emulsions in Water

Sodium dodecyl sulfate (SDS) [CH_3-$(CH_2)_{11}$-OSO_3^--Na^+] is an amphiphilic molecule which consists of a hydrophilic polar head and a hydrophobic non-polar tail. At high concentrations of SDS, SDS monomers aggregate into structure called micelles. A micelle is thermodynamically stable aggregation, where the non-polar tails are sequestered inward to avoid exposure to water, and the polar heads are oriented outward in contact with aqueous solution. This configuration avoids the contact of the hydrophobic tail with water, and minimizes the energy. The micelles can be made of a mixture of surfactants, for instance SDS and butanol. The butanol is called a cosurfactant. Figure 2.1 illustrates the SDS monomer; and SDS monomers formed micelle. SDS is used to stabilize the interface between two immiscible liquids. In this experiment, the two immiscible solutions that we used are α-eicosene dissolved chloroform and diluted SDS in deionized water.

Different concentrations of α-eicosene, 5 wt%, 2wt%, 500ppm, were prepared by dissolving each of them in chloroform. SDS was diluted with deionized water into a concentration of 20mM. These two solutions were prepared at our lab ambient

temperature, 22^0C. Other research conducted for emulsification that melted α-eicosene at 80^0C in a concentrated SDS solution [10].

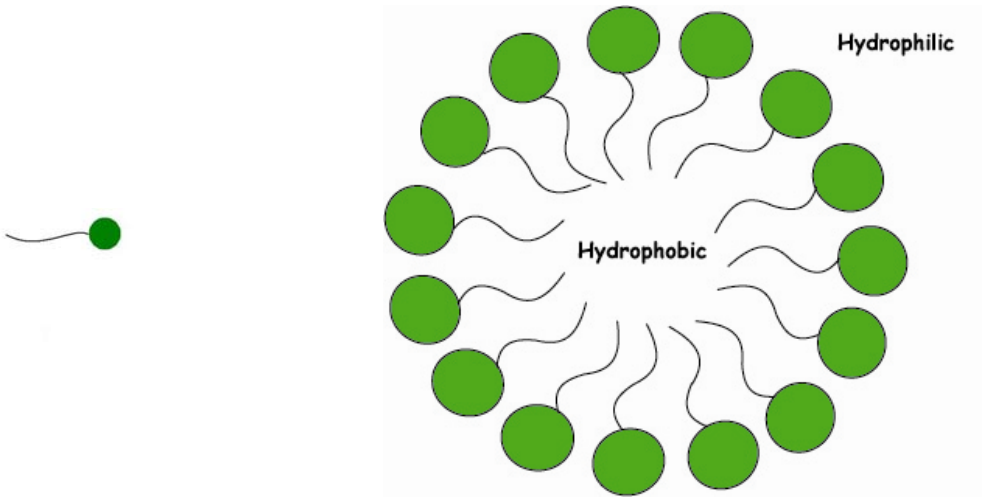

(a) (b)

Figure 2.1. Emulsification with surfactants. (a) Sodium dodecyl sulfate (SDS) monomer consists of a hydrophilic polar head and a hydrophobic non-polar tail. (b) SDS micelle formed by hydrophilic polar heads orienting outward in contact with water, and hydrophobic non-polar tails sequestering inward to avoid exposure to water.

Glass Microfluidic Device

We constructed our own microfluidic device which is made by glass, figure 2.2 shows the structure of the device. It consists of two glass capillaries, one is concentric and the other is square in shape, that allows SDS solution to flow from the outside of the inner capillary, and wax dissolved chloroform flow from the center position of the microfluidic device. Figures 2.3 and 2.4 sketch the microfluidic device's configurations and flow directions of the two solutions.

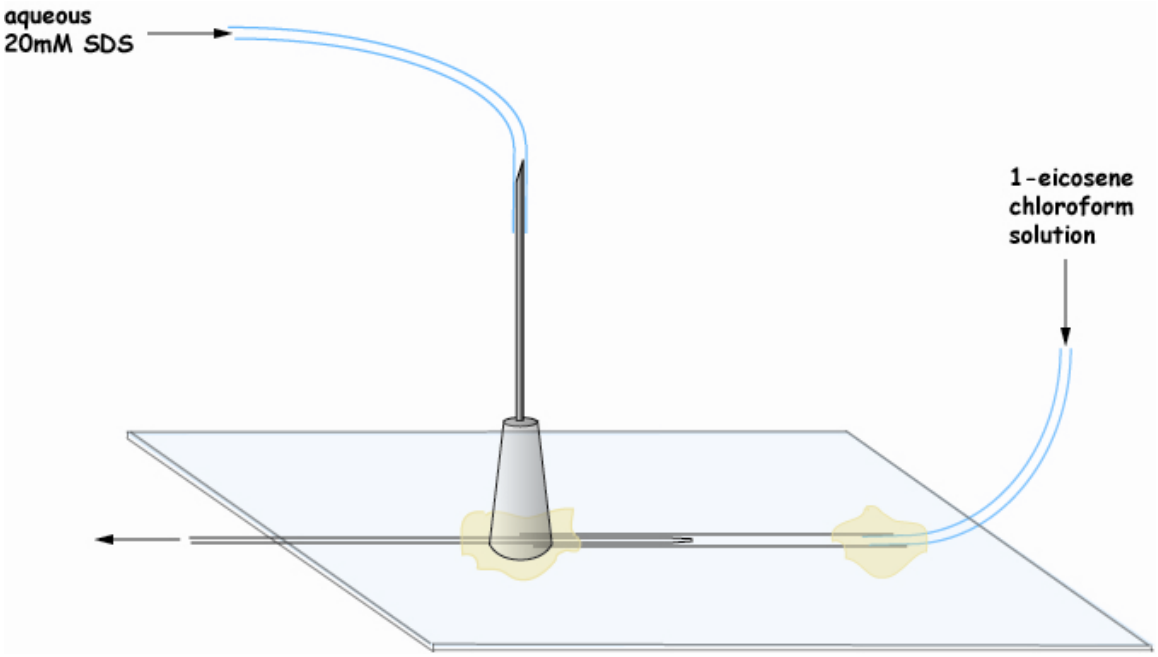

Figure 2.2. The glass microfluidic device was used in our experiments.

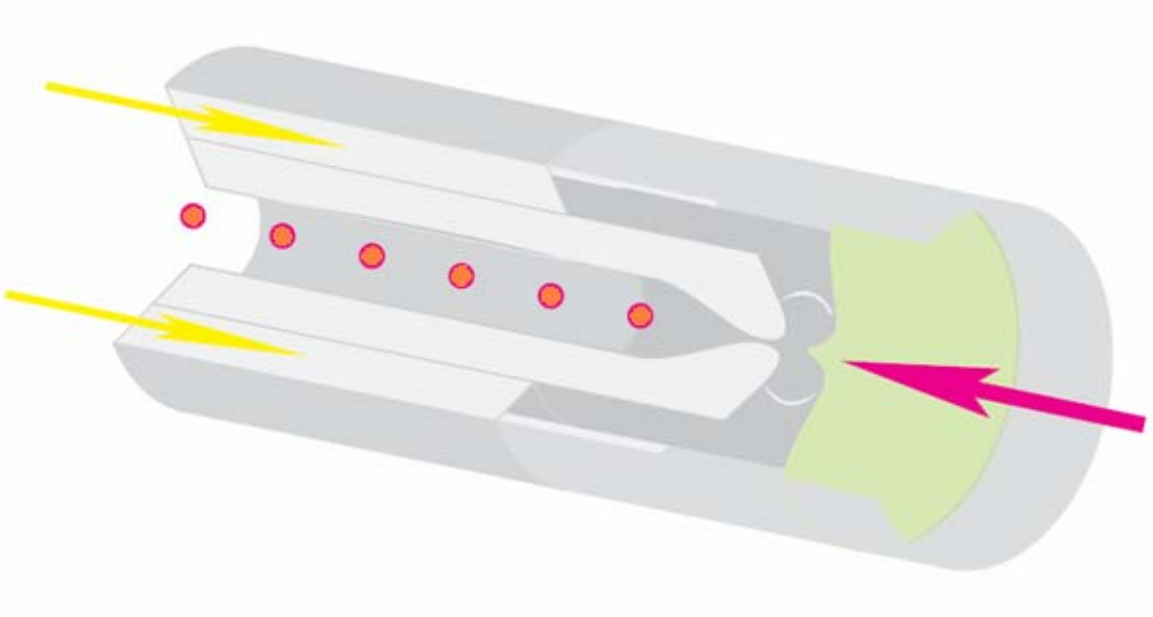

Figure 2.3. Cross-section of the microfluidic device. Red arrow shows the in-flow of the α-eicosene chloroform solution. Yellow arrows show in-flow of the SDS solution. Orange circles represent the chloroform emulsions produced. They are then collected at the exit end of the inner capillary.

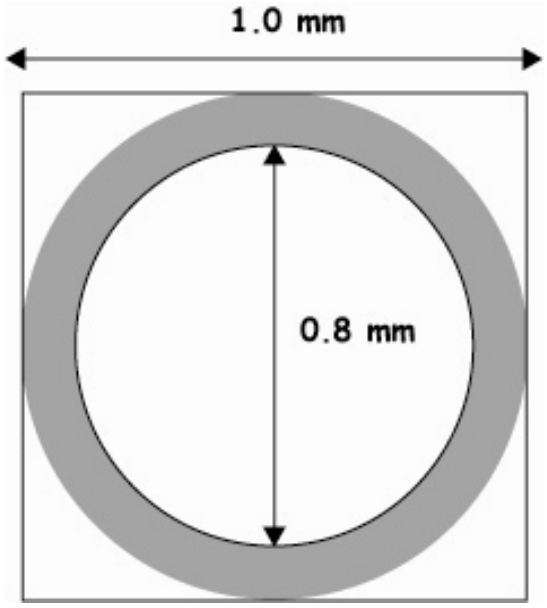

Figure 2.4. Cross-section of the capillaries. Outer 1.0 mm ID square capillary surrounds the inner round capillary which has a 0.80 mm ID and 1.0 mm OD. Emulsions are produced and collected in the round capillary. The space between the outer square capillary and the inner round capillary allows the solutions' laminar flow.

At the orifice of the inner capillary, uniform sized emulsions start to form when the flow of two solutions reach steady state. They are then collected at the end of the exit of the inner capillary and stored in a 20mM SDS solution. The SDS surfactants are used to help to stabilize the chloroform-water and wax-water interface.

This glass microfluidic device has several advantages. First, it can produce uniform size of droplets. Figure 2.5 shows the uniformity of the α-eicosene droplets that produced by this glass microfluidic device. Secondly, the size of the orifice and ratio of the flow rates of the two solutions can be manipulated, so that the size of the droplets can

also be controlled. Thirdly, this microfluidic device is three dimensional, it allows SDS solution to flow around the wax droplets and stabilize them against coalescence. Comparing to other microfluidic device, for example polydimethylsiloxane (PDMS) microfluidic device, it only works well for hydrophilic droplets in hydrophobic fluids. On the other hand, for our glass microfluidic device works well for both hydrophilic and hydrophobic droplets.

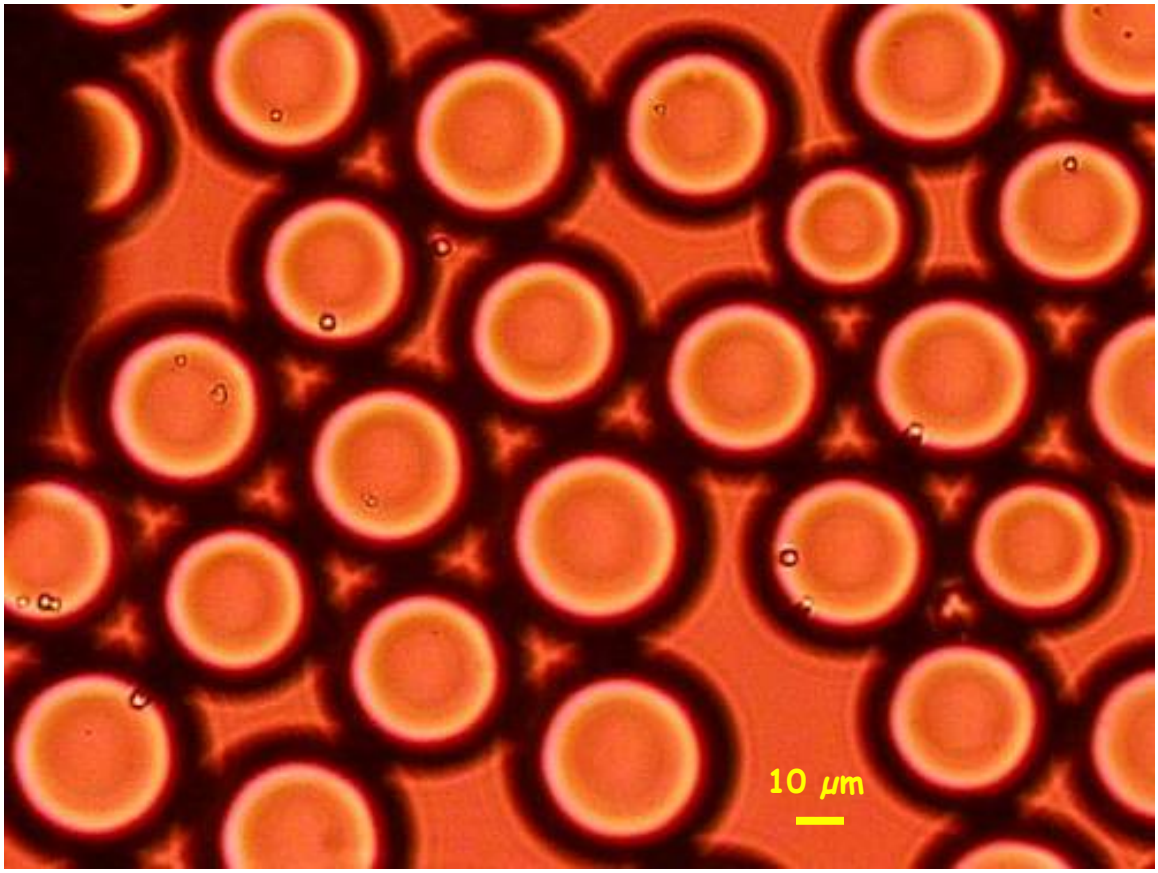

Figure 2.5. Uniform α-eicosene droplets are produced by the glass microfluidic device.

Droplets Evaporation

Before evaporation of chloroform, the droplets will stay at the bottom of the vial, since the density of chloroform (ρ = 1.498 g/cm^3) is much heavier than that of the aqueous SDS solution and α-eicosene [CH_2=CH-(CH_2)$_{17}$-CH_3]. In order to let the droplets undergo a temporal change in composition, chloroform evaporation is needed and which may lead to the formation of concentration gradients inside the droplets [11]. For evaporating quickly the chloroform out of the emulsions, surface evaporation has been chosen and carried.

Surface evaporation is performed on the glass surface at a temperature of 22^{o}C which is our laboratory's ambient temperature. After α-eicosene contained droplets are produced from the microfluidic device, they form a thin layer on top of a flat glass surface. Waiting until all droplets are dried, glass slides are then submerged into a beaker of 20mM SDS aqueous solution and put into an ultrasonic bath. All α-eicosene particles resulted from emulsion evaporation are washed away from the flat glass surfaces and then collected. Figure 2.6 shows the surface evaporation of α-eicosene in chloroform droplets is performed on the glass surface and 20mM SDS is surrounding the droplets.

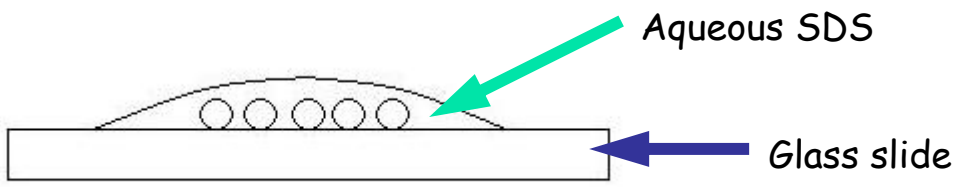

Figure 2.6. Surface evaporation of α-eicosene in chloroform droplets is performed on the glass surface. 20mM SDS is surrounding the droplets.

Evaporation of small droplets has also been studied in other research, which demonstrated a mechanism of flow generation within the droplets floating in denser oil [12]. They have established a FEMLAB simulation for hydrodynamic flows inside the droplet, which was in a good correlation with their experimental observations. Also, the internal circulation of evaporating the small droplets is found and which is driven by Marangoni instabilities [12].

The wax particles will cream up to the top of the aqueous solution due to the buoyant force, as the density of α-eicosene ($\rho = 0.795$ g/cm^3) is lighter than that of water. Some of the particles have shown birefringence as we observed them after surface evaporation but before cooling down in the refrigerator. This is because isotropic-smectic phase transition point of α-eicosene is around 26^{o}C [13], which is around the room temperature.

After collection, the wax particles are then stored in the refrigerator at a temperature of 3^{o}C in order to let the isotropic-to-smectic phase transition being carried

out. Figure 2.7 sketches the generation of disk-like particles from spherical particles as phase transition takes place from isotropic to smectic phase.

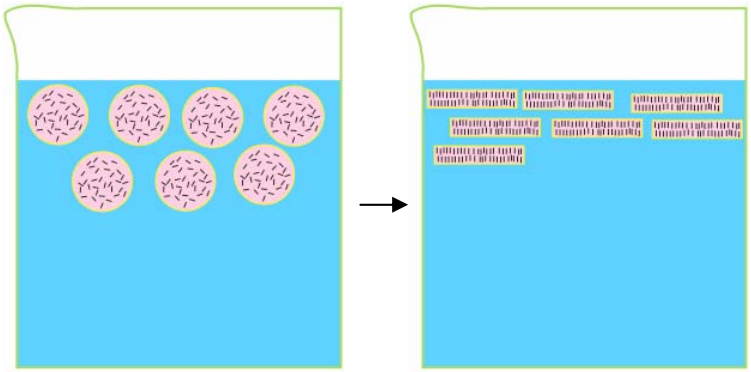

Figure 2.7. Generation of disk-like particles through isotropic-smectic phase transition.

Nucleation and growth occur in phase transition in which nuclei of a new phase are first formed, and then followed by the raising of the new phase at a faster rate. This process requires formation of new surface; therefore, surface free energy is a key parameter in which it is the energy required to create a surface. By varying pressure and temperature, phase change of a system can be initiated. In our daily life, cloud seeding, ice formation, or pop can fizzing are some of the examples of nucleation and growth. As we open a soda can, pressure is released and the bubbles of carbon dioxide float onto the top surface of the liquid and its size is increasing at the same time.

Nucleation is the beginning of a phase transition which nuclei are formed in solution. Increasing number of particles in nucleation depends on the liquid phase instability as temperature is decreasing, and so a driving force will be established toward equilibrium. Homogeneous nucleation is the condensation of a single chemical compound. Growth of the freshly nucleated particles is diffusion controlled. The size of particles is growing in this diffusive growth while the number of particles nucleated will stay nearly constant.

In order to analyze the processes of solvent evaporation and solute crystallization, models such as concentration profile in evaporating droplets have been developed. One of the investigations shows that increased drying temperatures lead to a decrease of bulk density of the dry particulate matter due to increased particle sizes [11].

In general, solute particle shape is determined by the number of nuclei nucleated and the growth of crystals. These are also influenced by the temperature and the solvent evaporation rate. Since the concentration of the solute is the highest at the surface of the solution droplets, crystallization was expected to initiate there [11]. Figure 2.8 presents the concentration profile in evaporating droplets. Droplet shrinks with time during evaporation, and at high evaporation rates large concentration gradients are formed.

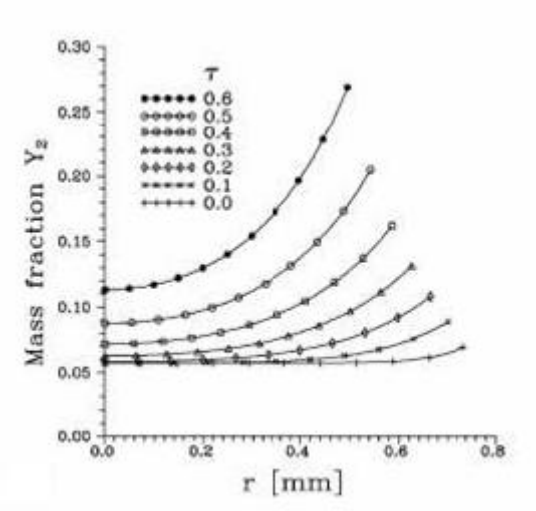

Figure 2.8. Concentration profile in evaporating droplets [11].

Spray drying is a process of generating droplets containing the required material in solution, and then to dry the particles until the solvent is completely removed, leaving a solid residue. Single crystal may be resulted when the solute concentration is low and the solubility is high; and crystallization occurs at a small size of droplet. On the other hand, multiple crystals will be resulted when the system is at a higher solute concentration and a lower solute solubility. To decrease the number of crystals formed, a decrease in nucleation rate, for example by lowering the rate of solvent evaporation, can be performed [14]. Hollow structured particle is formed when the particle has a large number of crystals, and because crystallization occurs at the surface, particles will be accumulated at the surface of the droplets. Cenospheres are formed as solute precipitates at the surface of the droplet. The size and density of cenosphere can be controlled by

lowering the solvent evaporation rate, so that the solute has more time to precipitate, and a more compact particle should be formed. A shell is formed by using a low solubility compound and high solvent evaporation rate. Also, when further drying of the shell, a collapsed cenosphere is formed. Figure 2.9 shows the morphology of particles obtained from spray drying of solution droplets [14]. This model is different from our model of disk-like particles formation from wax solution droplets evaporation, because this model is evaporating in the air while our system is evaporating under aqueous SDS medium. In addition, SDS can prevent aggregation of the wax droplets.

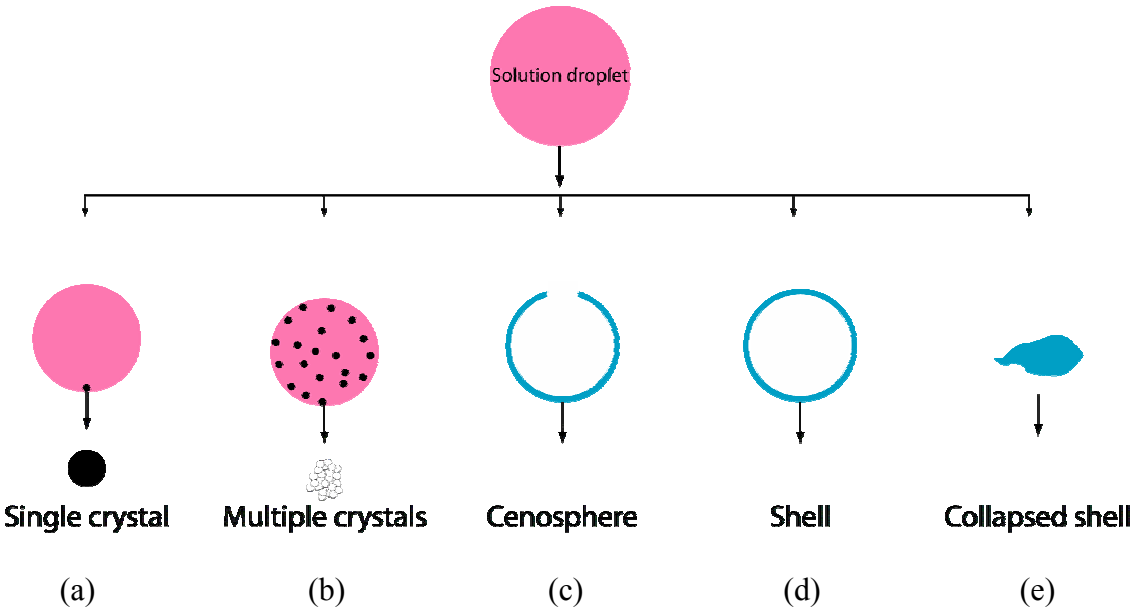

Figure 2.9. Possible modes of wax particle formation for spray drying. Formation of (a) single solid particle, (b) multiple particles, (c) cenosphere, (d) shell, (e) collapsed shell, as initial wax concentration increases [14].

Estimation of rate of chloroform evaporation under aqueous SDS medium is calculated by measuring the diameter of the wax droplet and the time elapsed during chloroform evaporation. Figure 2.10 demonstrates the sequential pictures of the freshly produced wax droplets that are taken at different time. These pictures are used to estimate the rate of chloroform evaporation in aqueous SDS medium by recording the diameters of the large wax droplet that is shown in the figure as time elapsed. As time is increasing, wax droplets are shrinking in size. By measuring the diameter of the wax particles, the rate of wax droplet shrinkage under aqueous SDS medium can be estimated. Figure 2.11 plots the diameters of the wax droplet against time under aqueous SDS medium, and the rate of chloroform evaporation is calculated by dividing the area of chloroform droplets, which assumes to be spherical in shape, shrinks as time elapsed. It is estimated to be $-7.634\times10^{-12}\,\frac{m^2}{s}$ for the larger size wax droplet that is shown in figure 2.11.

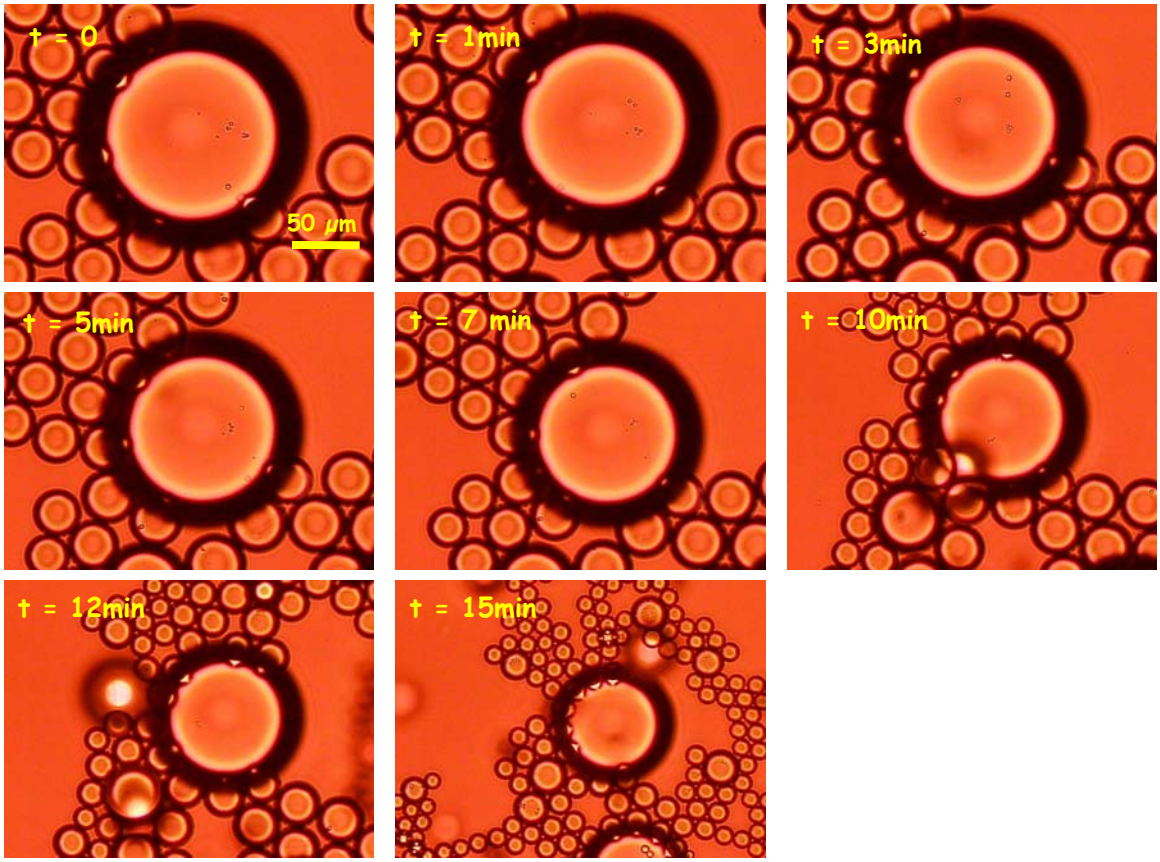

Figure 2.10. Estimation the rate of chloroform evaporation in aqueous SDS medium. As time increase, wax droplets are shrinking in size. By measuring the diameter of the wax particles, the rate of wax droplet shrinkage can be estimated.

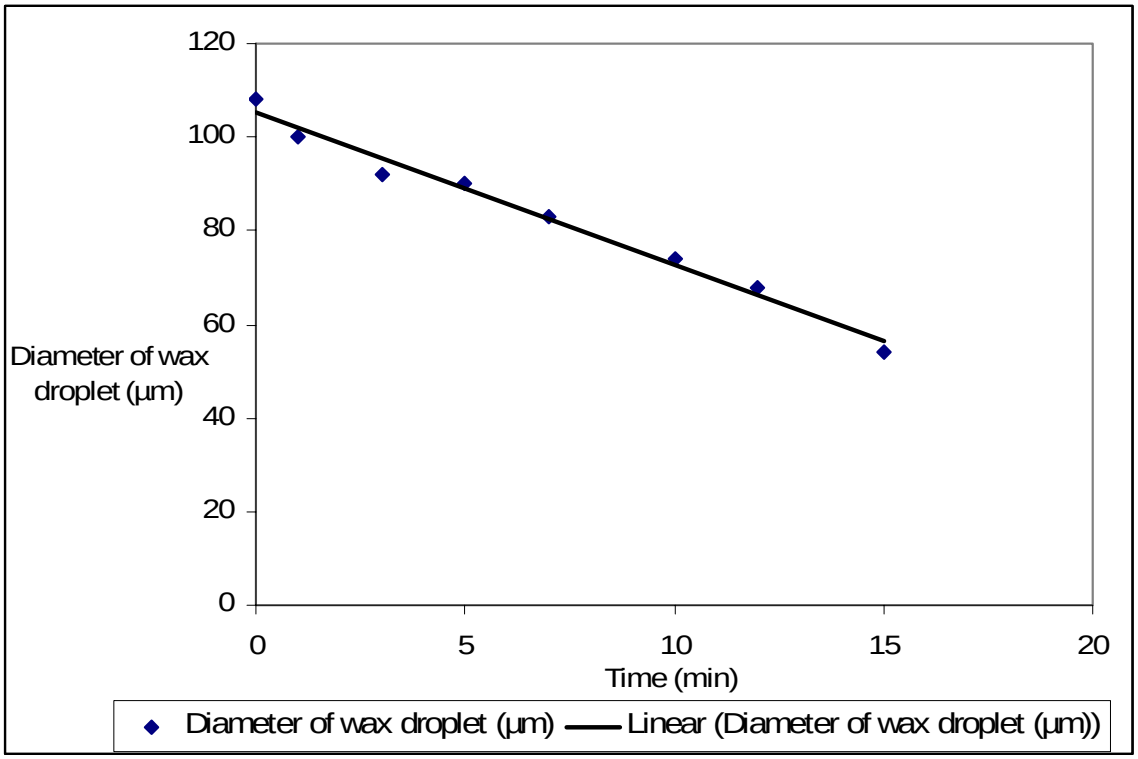

Figure 2.11. Diameter of initial concentration 5 wt% of wax droplet decreases during chloroform evaporation. Rate of chloroform evaporate is estimated to be $-7.634\times10^{-12}\,\frac{m^2}{s}$.

In order to determine the final number of wax particles formed during solvent evaporation, we used mass balance equation:

$$n_f \rho_f \frac{\pi}{2}\left(\frac{d_f}{2}\right)^3 = n_i \rho_i \frac{4\pi}{3}\left(\frac{d_i}{2}\right)^3 c$$

where the subscripts i and f represent the initial and final states; n is the number of wax particles; ρ is the density of α-eicosene; d is the diameter of α-eicosene particles; c is the initial α-eicosene in chloroform concentration. Assuming n_i is equal to 1, as wax droplets haven't started splitting into particles at time zero. Also, assume the initial and final α-eicosene density does not changed, and the aspect ratio for our system is equal to 4. Therefore, the mass balance equation reduced to:

$$n_f = \frac{8}{3}\left(\frac{d_f}{d_i}\right)^{-3} c$$

Figure 2.12 shows the plot of n_f versus the initial α-eicosene in chloroform concentrations. The higher the initial wax concentration, the more split wax particles are obtained. The result is consistent with the solution droplets drying morphology [14] into the multiple crystals model. The number of final number of wax particles split from the experimental observation is about 80,000.

Figure 2.13 sketches the model of disk-like particles formation from wax droplets evaporation. Uniform 50μm diameter wax contained chloroform droplets are firstly produced by the glass microfluidic device, they are then undergone chloroform evaporation. As solvent evaporates, nucleation and growth of wax droplets occurs at the surface of the droplets, since the wax molecules have a higher concentration there. And

finally, the wax droplets change into disks under the isotropic-smectic phase transition. We observed the wax droplets have a size change from the time just after the solvent evaporated, about 1μm, to the time as disk-like wax particles are formed, which are larger than 1μm in diameter.

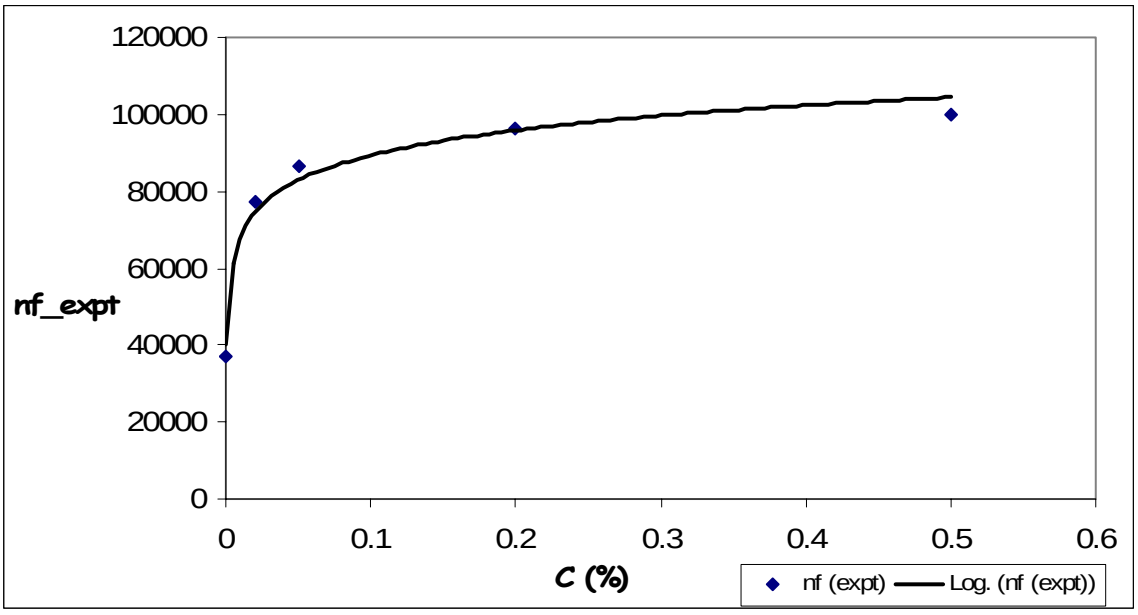

Figure 2.12. A plot of final number of wax particles formed, n_f, versus the initial α-eicosene in chloroform concentrations, c. It shows the higher the initial wax concentration, the more split wax particles are obtained.

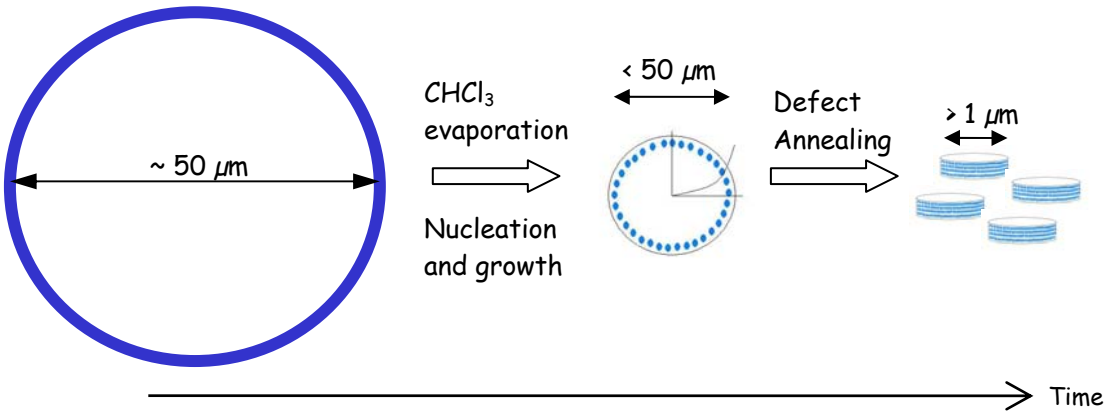

Figure 2.13. Model of disk-like particles formation from wax solution droplets evaporation.

CHAPTER III

WAX-DISK FORMATION

Anisotropic wax particles are formed after solvent evaporation. Nucleation and growth of the smectic phase occur, and caused the apparent size of the wax particles increase and finally the disk-shaped wax particles were generated. Disk-shaped wax particles morphology change is due to defect annealing. Since wax are in anisotropic smectic phase, they are birefringent and can be observed under the polarized light microscope.

Phase Transition

Transformation from phase to phase, for the first order transition such as crystallization, requires nucleation and growth of the new phase. Nucleation depends on whether the energy is allowed to be minimized thermodynamically such as the minimization of the Gibbs free energy, and also kinetically how fast the nucleation rate is.

Molecules always collide with each other. In general, molecules will have a lower energy when molecules are collided and stayed together, than further apart, if there is intermolecular attraction. Free energy is minimized when molecules are in crystal structure comparing to liquid. This energy difference is called volume free energy ($\rho\Delta\mu$), where ρ is the density of the bulk liquid, and $\Delta\mu$ is the chemical potential difference between the bulk solid and bulk liquid [15]. Solid grows in size, since the magnitude of the total volume free energy decreases. However, when solid forms in a liquid, an interface is

created in which a surface free energy γ is associated with it. As liquid phase transfer more into solid phase, total surface free energy increases. Lekkerkerker H.N.W. has shown that the classical theory of the free energy (ΔG) is: [15]

$$\Delta G = \frac{4}{3}\pi r^3 \rho \Delta\mu + 4\pi r^2 \gamma$$

where the first term deals with the bulk free energy change, and the second term deals with the surface free energy change. Both terms are involved in the energy minimization and the phase transitions.

When liquid is cooled, only a few molecules will stick together at the freezing point, because they still have comparatively high energy. As liquid further cooled, much more nuclei are formed. When the number of nuclei is large enough, the supercooled liquid will quickly change into a solid by the growth of the crystallites. This process is called homogeneous nucleation and growth. It usually occurs when the material is highly pure.

Particle Morphology Change Due to Defect Annealing

After the wax particles nucleated, they start to grow in size with time. When the system is cooled through the transition temperature, the disk-like wax particles formed. Domain changes inside the particles dictate the dynamics of disk-like shape formation. Coarsening of domains can be described by the power-law: $L \propto t^n$ describes the shape change; where L is the characteristic length of the wax particles size, t is the time and n is the growth exponent [16]. Research [17] has been studied for the coarsening in foams made from the pure liquid crystal, 8CB (4-n-octylcyanobiphenyl), without the presence of any

solvent or surfactant, its growth exponent (n) of it is $\approx 0.20 \pm 0.05$. For our experiment, the data obtained for 500ppm, 2 wt% and 5 wt% of the initial wax concentrations dissolved in chloroform, the growth exponents are 0.278, 0.147 and 0.145 respectively. Graphical results are shown in the later section (figure 3.18, section 4). The smaller the size of the particle, the faster its dynamics is. The mechanisms for coarsening in different phases are influenced by the material flow in domains and the growth of domain size by the flow from small domains and integrate into larger domains.

In smectic phase, wax molecules arranged into fluid layers with perpendicular orientation. Theoretically, layers are perfectly parallel to the free surfaces. Due to the domain defects the particle looks spherical even in smectic phase. The shape of liquid crystals changes from spherical to disk-shaped particles with decreasing domain defects, moreover, the wax disks formation is a defect annealing process. As in liquid crystal annealing, the apparent size of the wax particles grows. Figure 3.1 shows the focal conic domains that appear in smectic phase. When the focal conic domains in smectic phase orient themselves into a sphere, their apexes are pointing into the center of the sphere while their circular top portions are facing outward. Furthermore, hexagonal shaped wax particles were also observed in which their formation is due to the defect annealing. When they observed under the polarized light microscope, the birefringent characteristic is shown at their edges. Figure 3.2 illustrates the hexagonal shaped wax particles are observed from the initial concentration 500ppm of α-eicosene in chloroform after 3 days refrigeration.

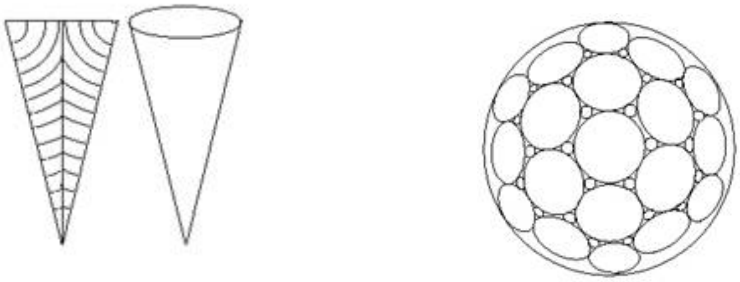

(a) (b)

Figure 3.1. Focal conic domains in smectic phase. (a) A cross-section of a focal conic domain. (b) When the focal conic domains orient themselves into a sphere, their apexes are pointing into the center of the sphere while their circular top portions are facing outward.

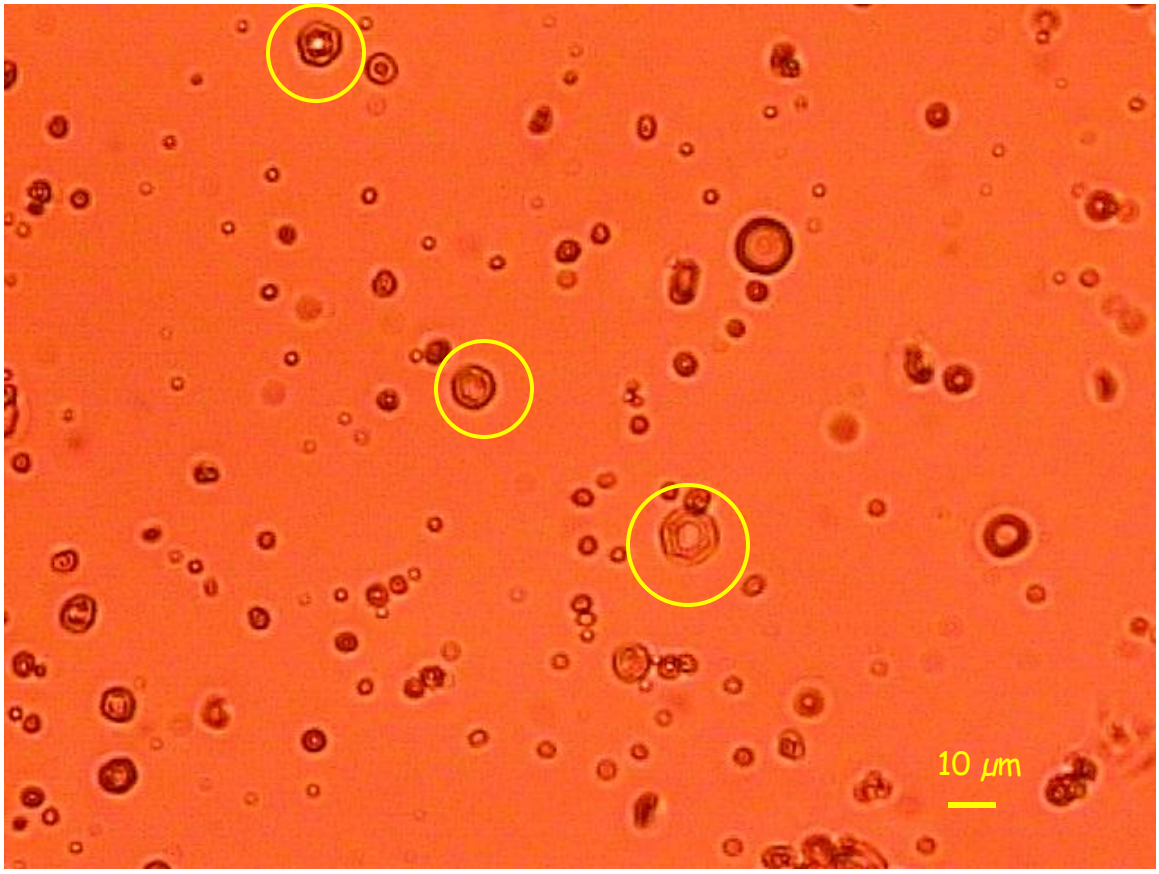

Figure 3.2. Hexagonal shaped wax particles are observed from the initial concentration 500ppm of α-eicosene in chloroform after 3 days refrigeration.

Birefringence of Liquid Crystals

Birefringence is one of the salient characteristics of liquid crystals, and it occurs in anisotropic phases: nematic, smectic, and crystalline phases. Liquid crystals experience birefringence due to the orientation characters, alignments and shapes of their molecules. Optical axis is the straight line passes through the centers of curvature of the lens surfaces, and when light travels along this axis would not be deflected in any direction. The electric field is everywhere perpendicular to the optical axis, and it is called the ordinary (o-) ray. Ordinary ray travels at the same velocity in every direction through the anisotropic materials. The light wave with the electric field parallel to the optic axis is called the extraordinary (e-) ray. Extraordinary ray travels at a velocity that depends on the propagation direction within the anisotropic materials. Birefringence defines as the difference in refractive indices, $\Delta n = n_e - n_o$, between the ordinary (n_o) and extraordinary (n_e) rays [18]. The retardation between the ordinary and extraordinary ray increases with increasing the anisotropic material's thickness [19]. One of the methods to determine birefringence is performed by F.N. Ecevit [20] using the continuous wavelet transform (CWT).

Because of the birefringence of the smectic phase appears inside the disks, they are observed under the polarized light microscope as shown in figures 3.3 to 3.14.

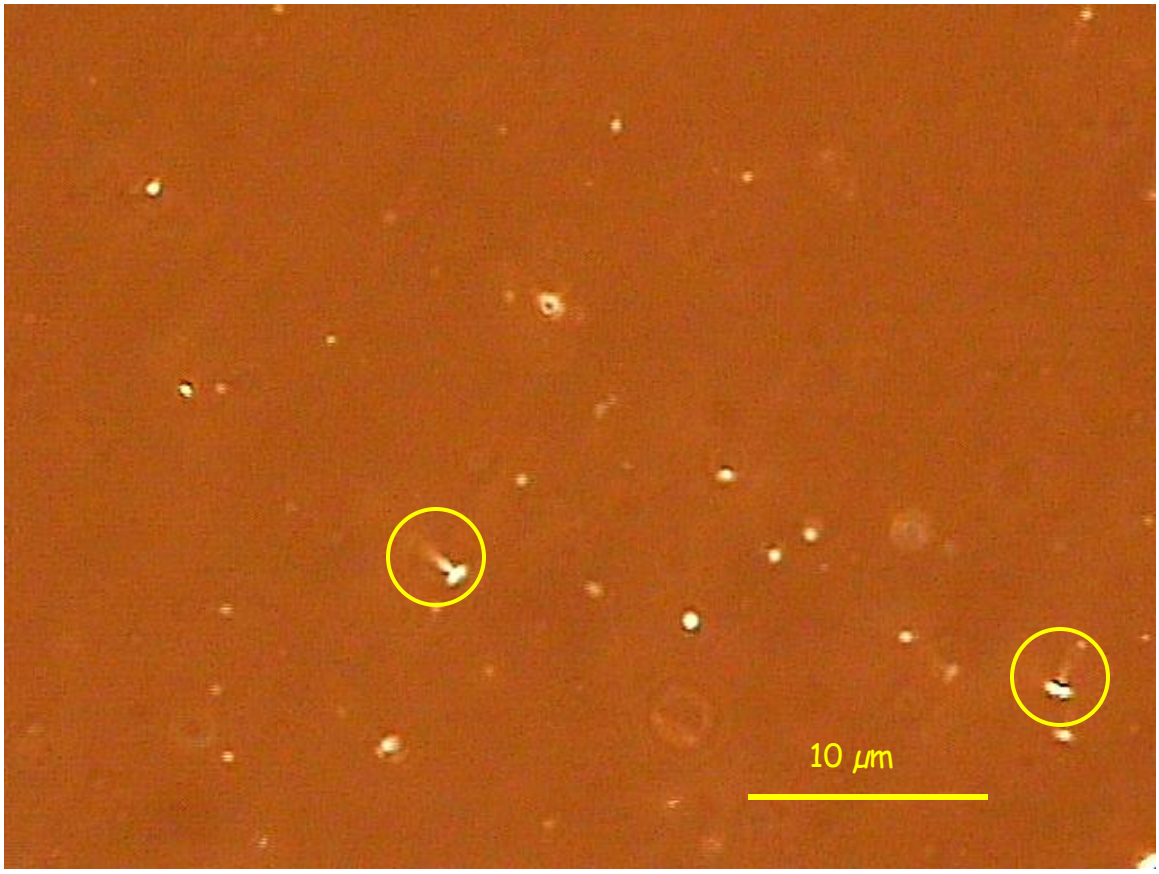

Figure 3.3. Wax particles are produced from the initial concentration 5 wt% of α-eicosene in chloroform after 3 days refrigeration. The micrograph was taken using a polarized light microscope. Diameter of the α-eicosene disks on average is about 1.22μm.

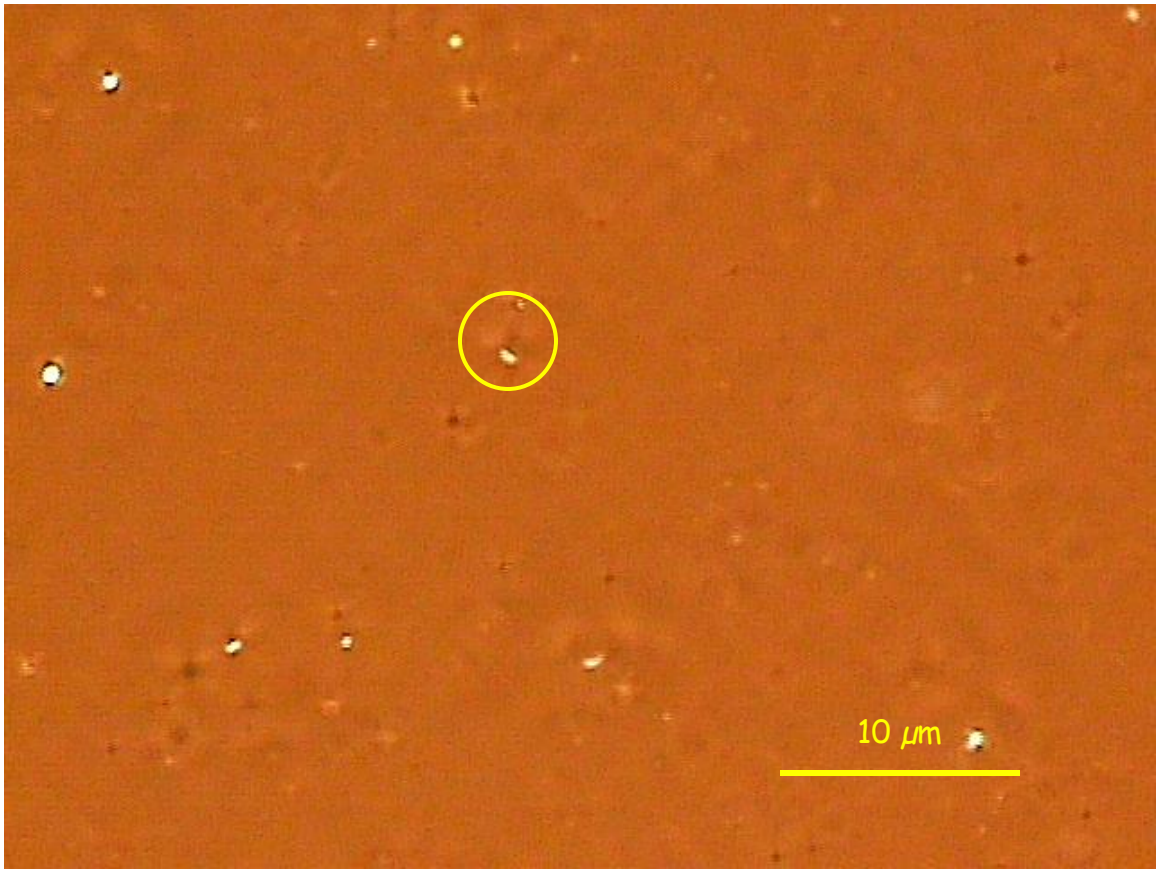

Figure 3.4. Wax particles are produced from the initial concentration 5 wt% of α-eicosene in chloroform after 13 days refrigeration. The micrograph was taken using a polarized light microscope. Diameter of the α-eicosene disks on average is about 1.22μm.

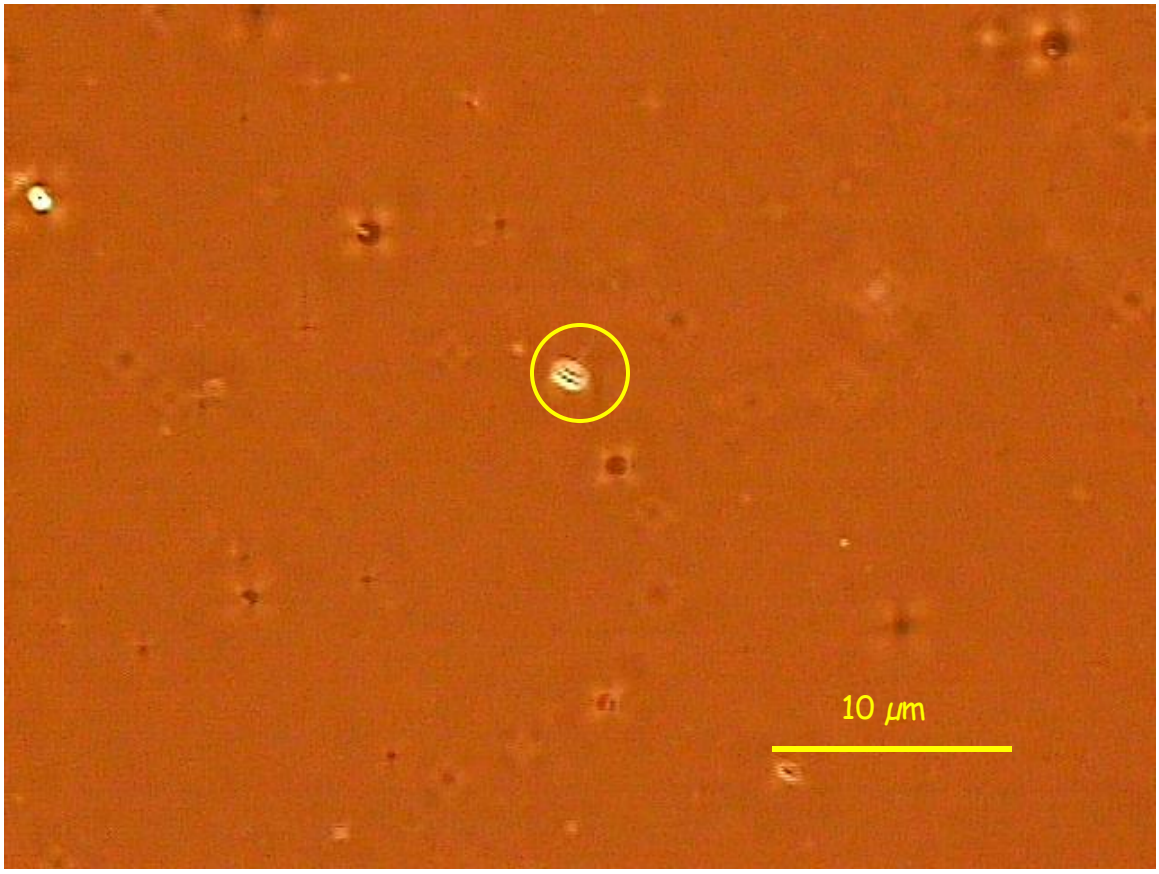

Figure 3.5. Wax particles are produced from the initial concentration 5 wt% of α-eicosene in chloroform after 23 days refrigeration. The micrograph was taken using a polarized light microscope. Diameter of the α-eicosene disks is about 1.43 - 1.84μm.

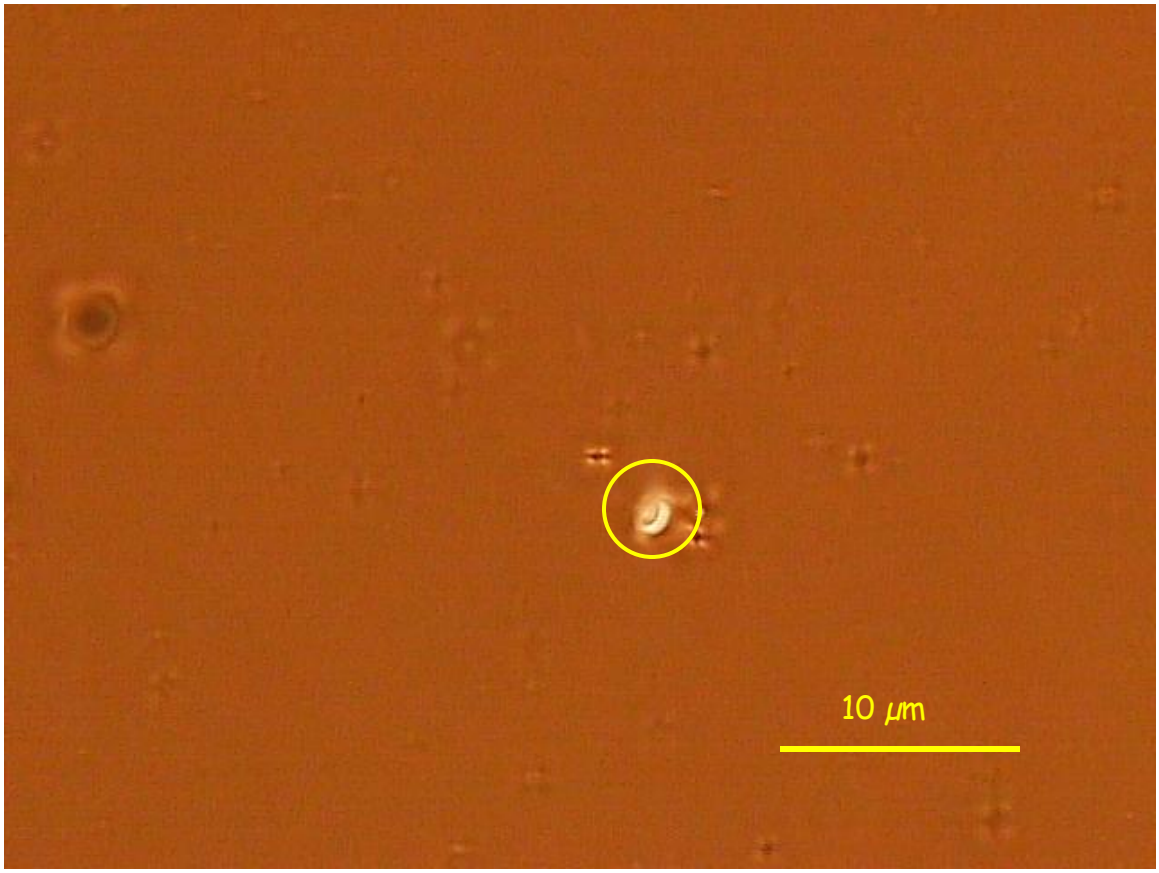

Figure 3.6. Wax particles are produced from the initial concentration 5 wt% of α-eicosene in chloroform after 42 days refrigeration. The micrograph was taken using a polarized light microscope. Diameter of the α-eicosene disks on average is about 2.04μm.

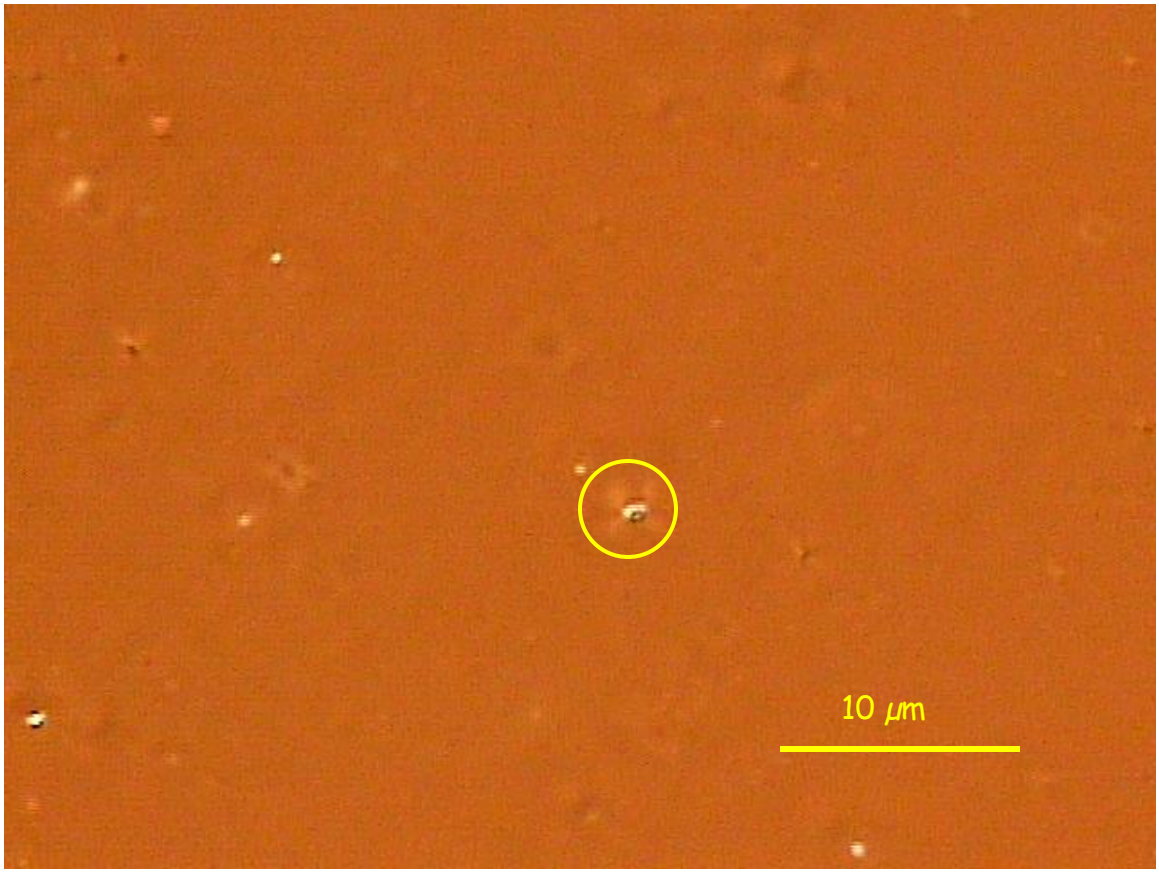

Figure 3.7. Wax particles are produced from the initial concentration 2 wt% of α-eicosene in chloroform after 13 days refrigeration. The micrograph was taken using a polarized light microscope. Diameter of the α-eicosene disks on average is about 1.43μm.

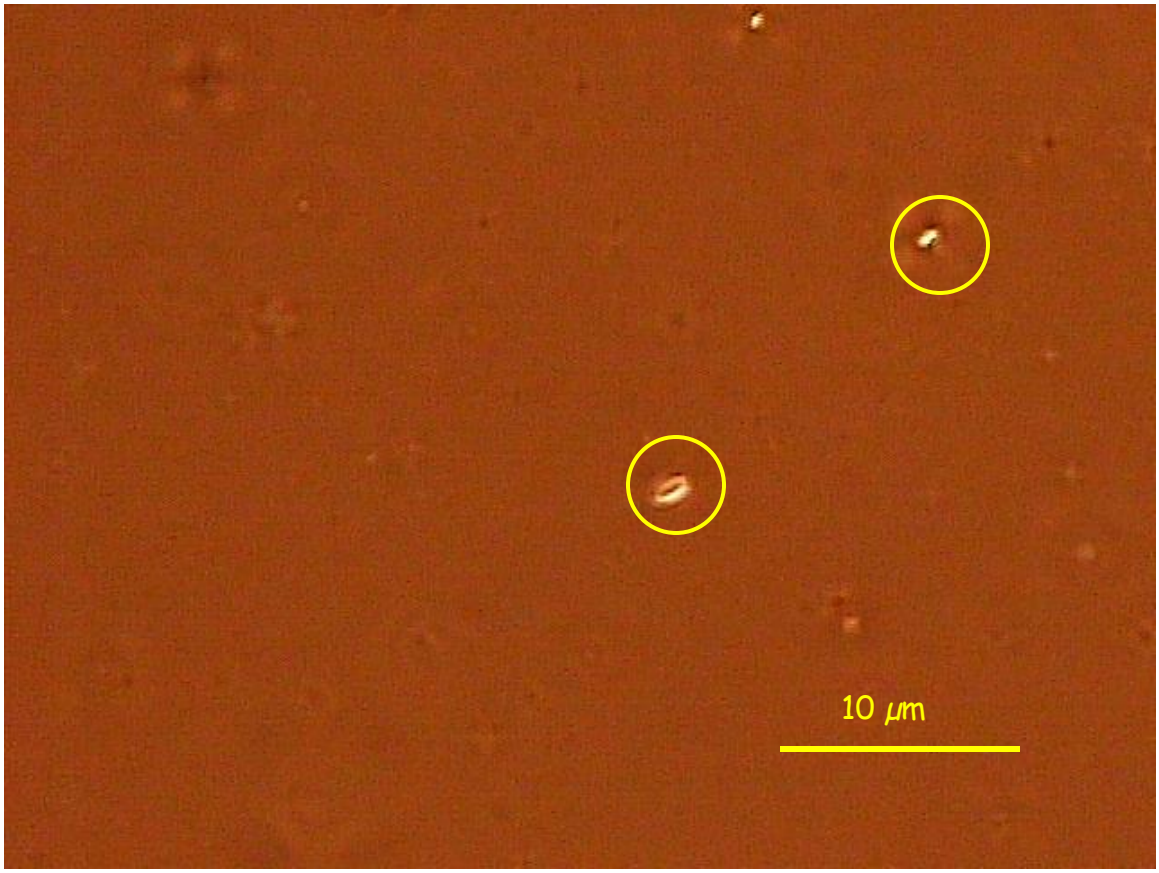

Figure 3.8. Wax particles are produced from the initial concentration 2 wt% of α-eicosene in chloroform after 22 days refrigeration. The micrograph was taken using a polarized light microscope. Diameter of the α-eicosene disks on average is about 1.63μm.

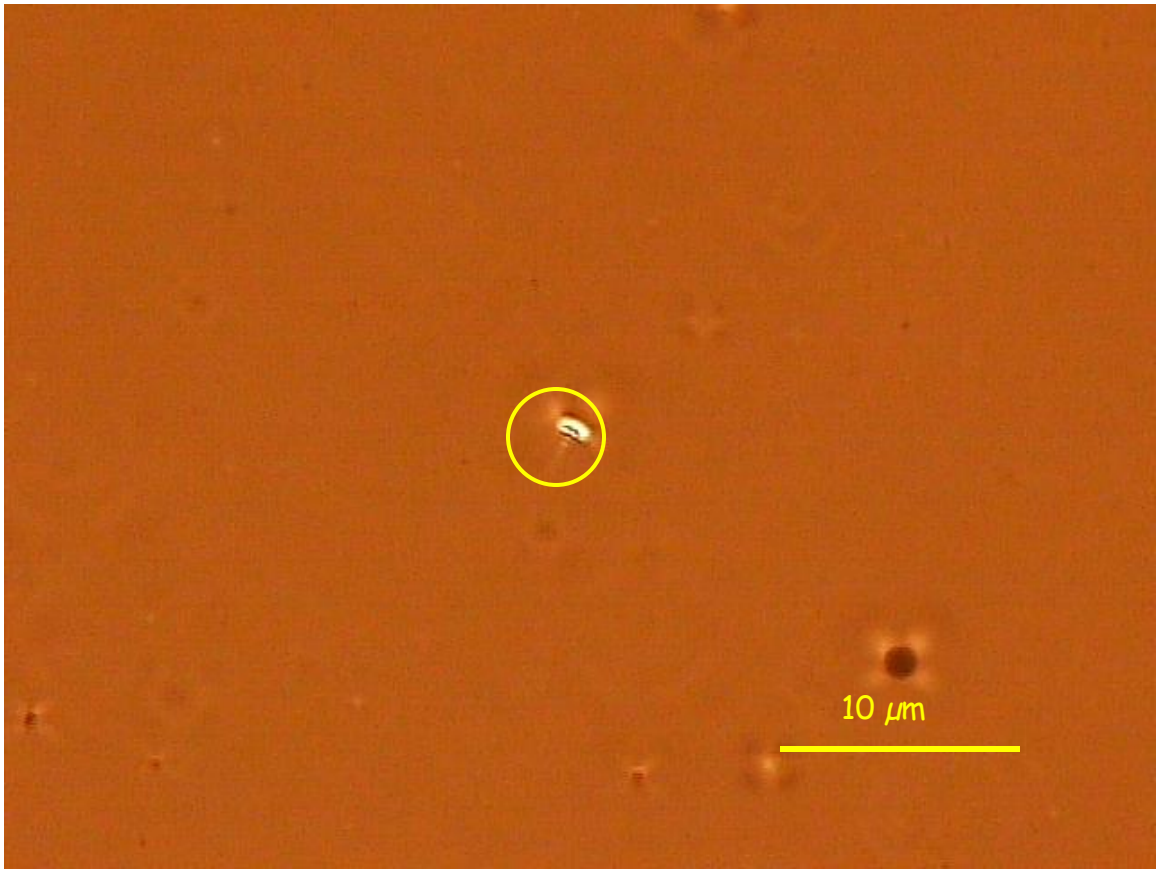

Figure 3.9. Wax particles are produced from the initial concentration 2 wt% of α-eicosene in chloroform after 47 days refrigeration. The micrograph was taken using a polarized light microscope. Diameter of the α-eicosene disks on average is about 1.70μm.

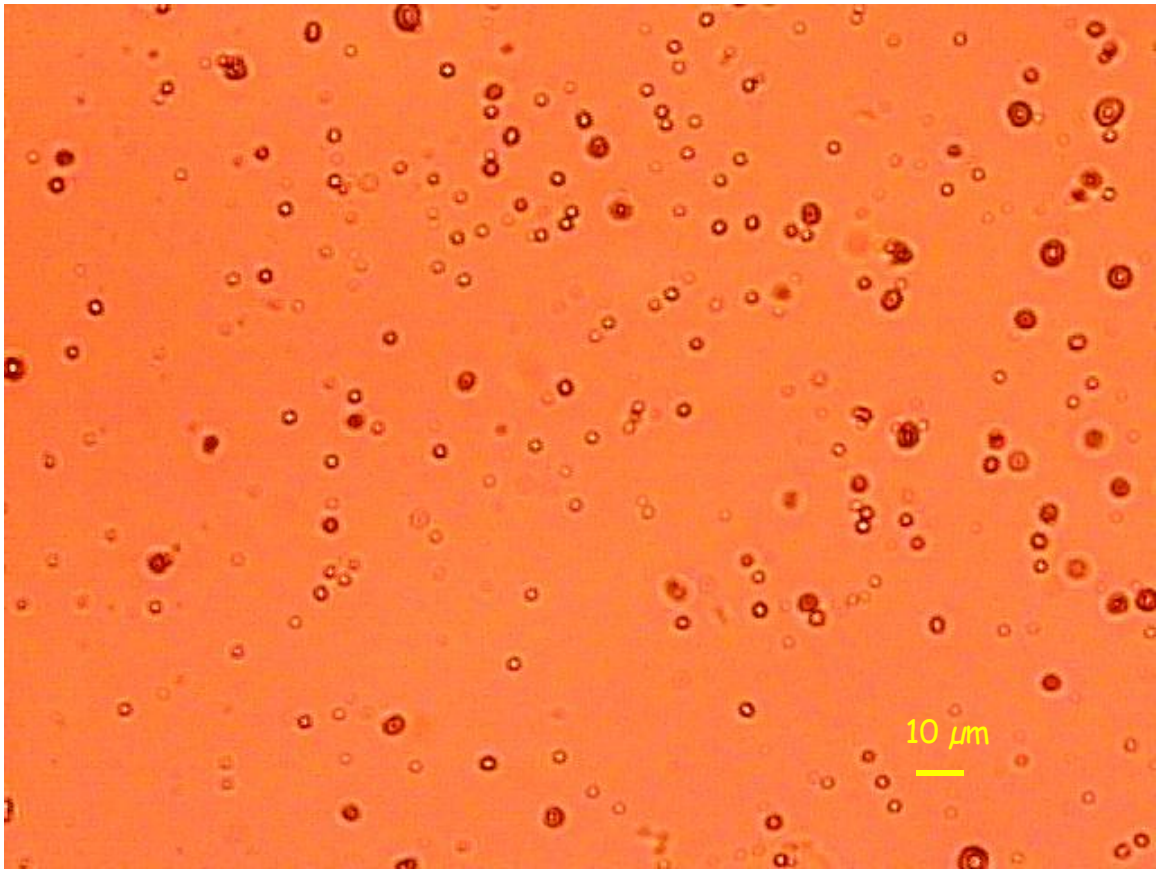

Figure 3.10. Wax particles are produced from the initial concentration 500ppm of α-eicosene in chloroform after 9 days refrigeration observed under the microscope without using the polarizers.

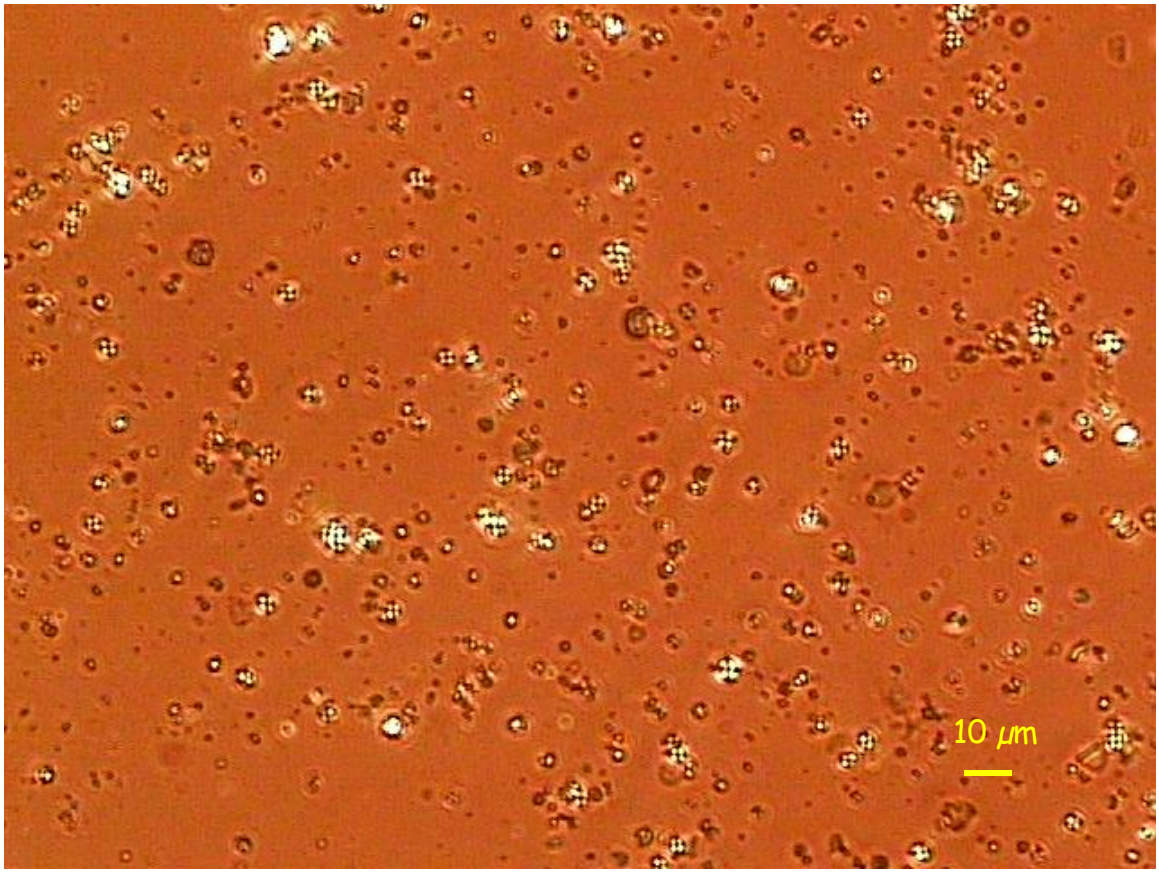

Figure 3.11. Wax particles are produced from the initial concentration 500ppm of α-eicosene in chloroform after 9 days refrigeration observed under the polarized light microscope.

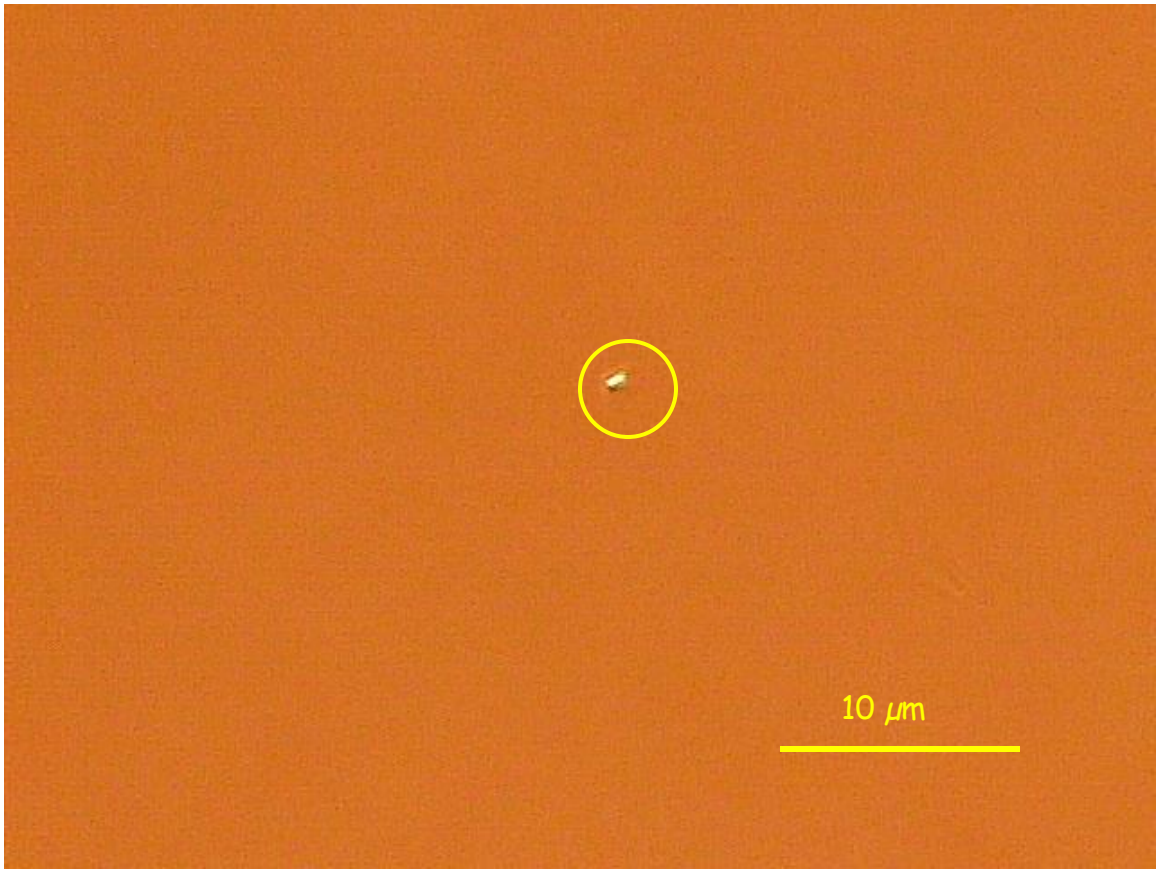

Figure 3.12. Wax particles are produced from the initial concentration 500ppm of α-eicosene in chloroform after 12 days refrigeration. The micrograph was taken using a polarized light microscope. Diameter of the α-eicosene disks on average is about 0.90μm.

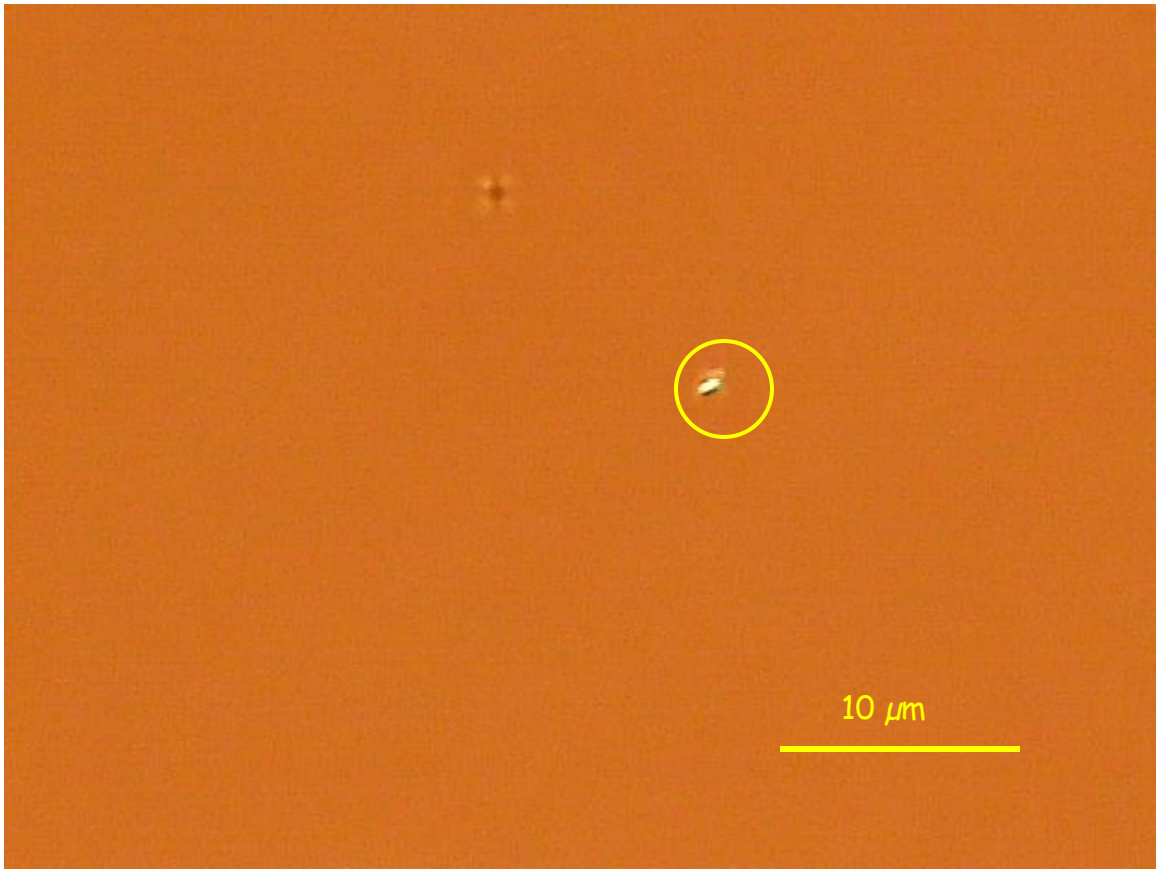

Figure 3.13. Wax particles are produced from the initial concentration 500ppm of α-eicosene in chloroform after 28 days refrigeration. The micrograph was taken using a polarized light microscope. Diameter of the α-eicosene disks on average is about 0.94μm.

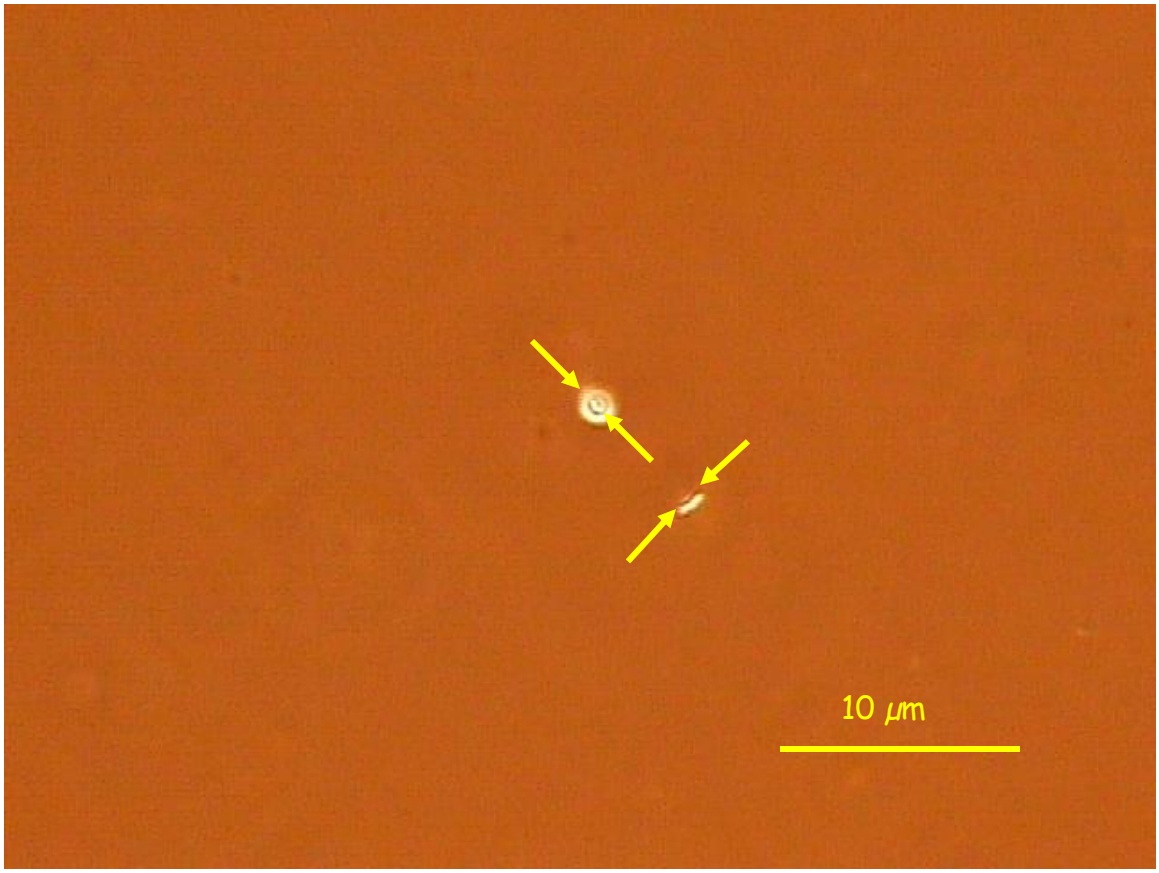

Figure 3.14. Wax particles are produced from the initial concentration 5 wt% of α-eicosene in chloroform after 2 months refrigeration. It shows the diameter and thickness of the α-eicosene disk is about 1.43μm and 0.32μm respectively, that is, the aspect ratio is 4. The diameter and thickness measurements of the disks are pointed out by the yellow arrows.

Observing the Wax-Disks

Due to the Brownian thermal forces [7], microdisks are fluctuating in different orientations. For observing the wax microdisks in our laboratory, an inverted polarized light microscope (Nikon TE2000-U) was used. Figure 3.15 demonstrates the configuration of the inverted polarized light microscope. The polarized light microscope can distinguish between isotropic and anisotropic materials, and investigate the structure and composition of materials.

Isotropic materials demonstrate the same optical properties in all directions, as they have only one refractive index and allow all vibration directions of light passing through them. When light enters an isotropic material, it is refracted at a constant angle and passes through the material at a single velocity without being polarized by interaction with the electronic components of the crystalline lattice. On the other hand, anisotropic materials have crystallographically distinct axes and act as beam splitters. Also they interact with light in a manner that is dependent upon the orientation of the crystalline lattice with respect to the incident light. When light enters along the optical axis of anisotropic crystals, light is refracted at a constant angle and passes through the material at a single velocity, which has the manner as the interaction with isotropic materials [19]. However, when light enters a non-equivalent axis, it is refracted into two rays, which are polarized, orientated at right angles to one another, and traveled at different velocities. This is called double refraction.

Polarized light microscope consists of two polarizing filters in the light path called polarizer and analyzer, as shown in figure 3.15. When both the polarizer and

analyzer are in the optical path, their polarization directions are positioned at a certain angle to each other. When the polarizer and analyzer are crossed at right angles to each other and an isotropic media is between them, no light is passing through the system and a dark field of view present in the eye piece.

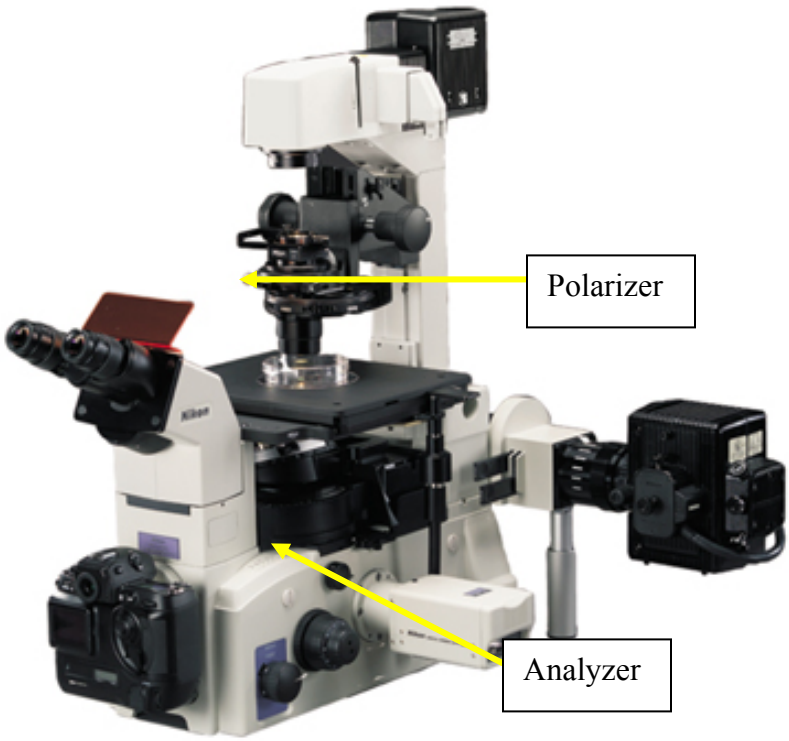

Figure 3.15. Inverted polarized light microscope (Nikon TE2000-U) used in our laboratory. A polarizer and an analyzer are installed in this microscope as shown by the yellow arrows.

When normal light rays first pass through the polarizer, part of the light rays will be absorbed, and the transmitted light rays will be polarized, meaning light only vibrates at one single direction. Figure 3.16 demonstrates the light rays passing through the birefringent material under the polarized light microscope. The transmitted light rays then pass through the anisotropic crystal where light rays are refracted and divided into two different components which are vibrating parallel to the crystallographic axes and perpendicular to each other. That is because the liquid crystal molecules have their own orientations and alignments; they observed differently of the light ray. Depending on the phases or the molecules' orientations of liquid crystals, the polarization of the transmitted light rays will be altered again after passing through the liquid crystals. The polarized light rays after passing through the birefringent material are then passed through the analyzer, which is oriented to pass a polarized vibration direction perpendicular to that of the polarizer, hence, the analyzer passes only those components of the light rays that are parallel to the polarization direction of the analyzer. As one of the waves is retarded compared to the other, interference occurs between the waves as they pass through the analyzer. Therefore, bright colors can be seen when observed through crossed polarizers. The wax molecules inside my anisotropic wax disks are in the smectic phase at room temperature around 22^0C. They are birefringent and can be observed under the polarized light microscope. In addition, polarized light microscope requires strain-free objectives and condensers to avoid depolarization effects on the transmitted light [19].

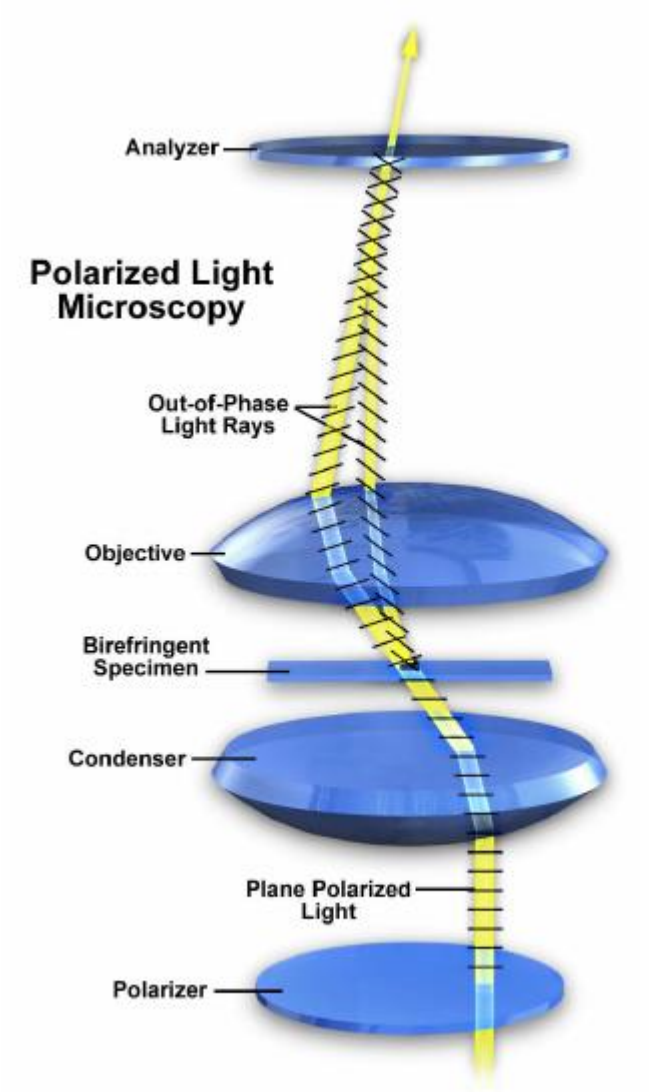

Figure 3.16. A systematic sketch of the polarized light microscopy.

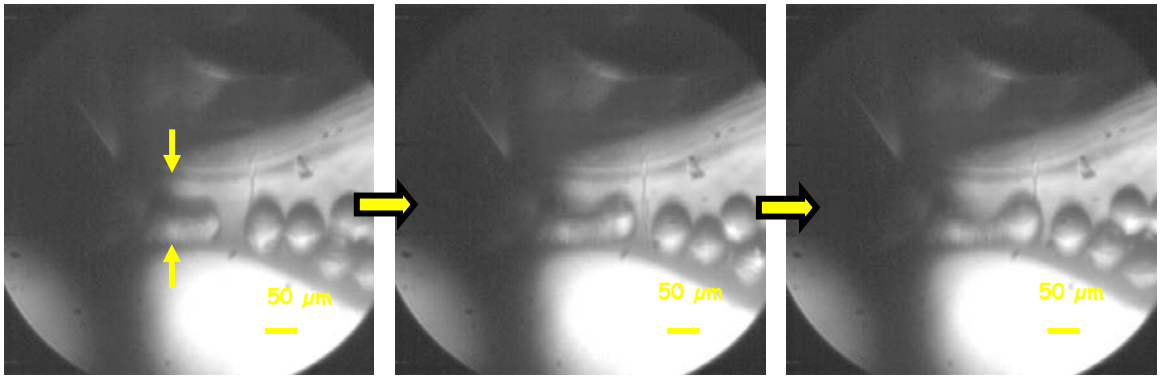

Figure 3.17. α-eicosene contained chloroform droplets are initially produced in the glass microfluidic device. Diameter of the cuvette opening is about 100 μm (as shown by the two yellow arrows). Size of the spherical emulsions is about 50 μm, and they are uniform in size due to the steady operation state.

The size and the shape of the microdisks are analyzed. Figure 3.17 shows initially 5 wt% α-eicosene in chloroform microemulsions were freshly produced in the microfluidic channel, and the size of the spherical emulsions is about 50μm in diameter. They are then transferred on the flat glass surface to evaporate the chloroform, and they are split into about 1μm to 2μm particles after chloroform has been observed to evaporate out. Figure 3.3 to 3.14 show different size of the α-eicosene particles vary with different initial α-eicosene concentrations as the refrigeration days increases. Figure 3.14 shows that the particles from the initial concentration 5 wt% of α-eicosene in chloroform after 2 months refrigeration has a diameter and thickness of 1.43μm and 0.32μm respectively. Therefore, the aspect ratio is about 4 (diameter of wax disk: thickness of wax disk). For 2 wt% α-eicosene disks after 47 days refrigeration shows the aspect ratio is also about 4; the diameter and thickness on average are found out to be about 1.70μm and 0.41μm respectively.

With all the data that we obtained from the experiments, the correlation between the size of wax particles and the time that the wax particles samples are stored in the refrigerator was plotted. Figure 3.18 shows the increasing size of the wax-disks as time increases. It is because the wax particles in isotropic phase are changing into wax disks in smectic phase and the molecules of the wax are orienting themselves into layers, that causes the aspect ratio, which is about 4, is observed. The aspect ratio increases as the wax particles are changing into disks. Moreover, birefringent occurs at the early time which means the phase transition from isotropic to smectic phase is fast. In order to produce disks, defect annealing takes place between domains in smectic phase.

The power-law is fitted into each set of data, and they have a trend of decreasing the growth of the wax particles as the initial wax concentration increases. Besides, the disk populations of different initial wax concentrations are also plotted. Figure 3.19 shows the wax disks population for different initial concentrations as the time of samples stored in the refrigerator increases. The disk populations were estimated by observing the disk-like wax particles which appear to be birefringent under the polarized light microscope.

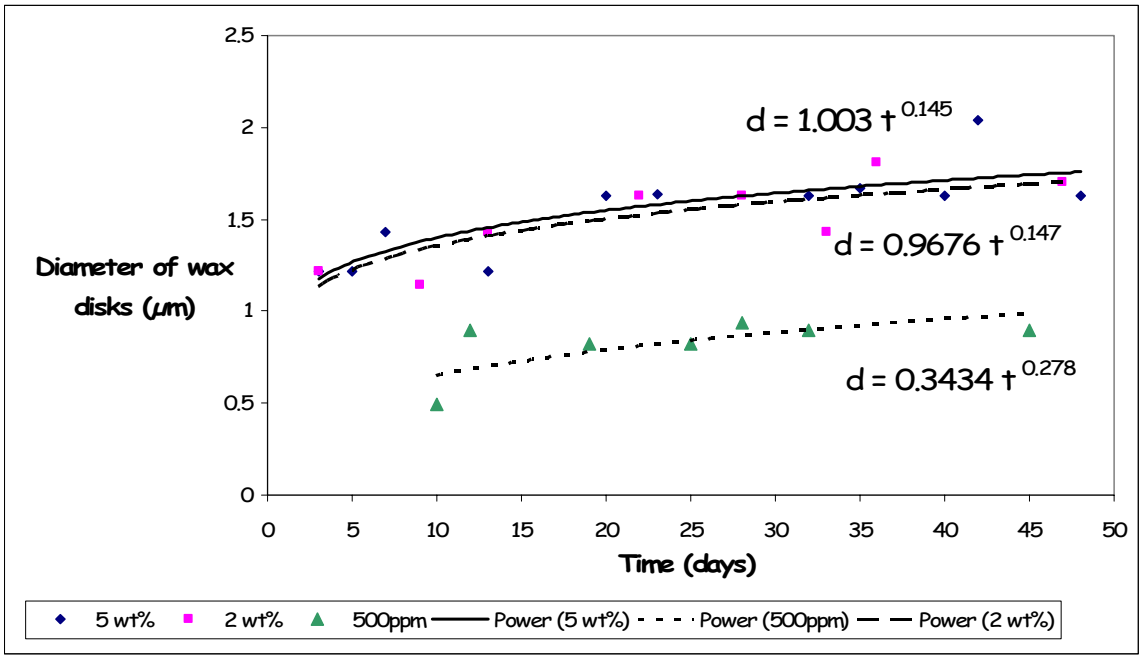

Figure 3.18. Size of wax-disks for 5 wt%, 2 wt% and 500ppm initial concentrations plotted against days of samples stored in the refrigerator.

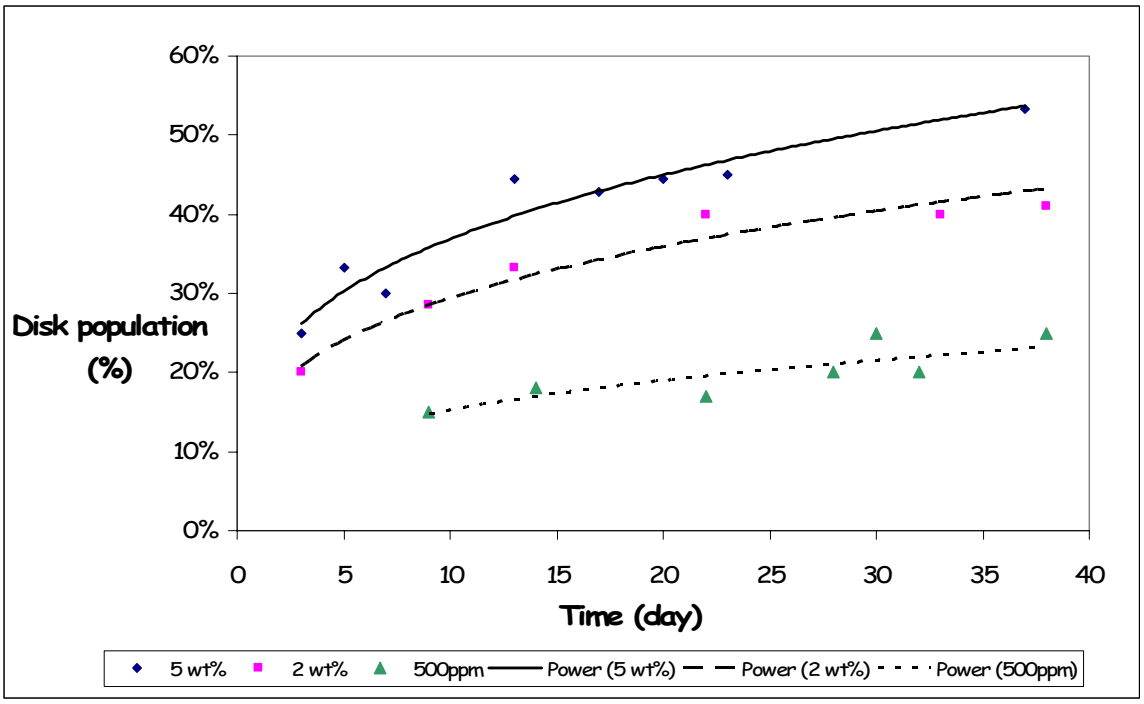

Figure 3.19. Wax-disk population for 5 wt%, 2 wt%, 500ppm initial concentrations plotted against days of samples stored in the refrigerator.

CHAPTER IV

DYNAMIC LIGHT SCATTERING AND DIFFUSIONS OF WAX DISKS

Dynamic Light Scattering (DLS)

Dynamic light scattering (DLS) is a common spectroscopic technique using in colloidal science. It measures the fluctuations in the scattered light intensity (I) arising from the motion of the sample [21]. For light scattering, the incident photon induces an oscillating dipole in the electron cloud. As the dipole changes, energy is scattered in all directions. When the size of particles is large compared to the wavelength of the incident light, the scattered pattern becomes extremely complex [21] and the intensity is angle dependent. If the light is coherent and monochromatic, as from a laser for example, it is possible to observe time-dependent fluctuations in the scattered intensity using a suitable detector such as a photomultiplier. Besides, DLS has a high sensitivity for small concentration of sample, and very small amount is required for scattering.

In analyzing the time dependence of the intensity fluctuation can yield the diffusion coefficient (D) of the particles by using the Stokes Einstein equation:

$$D = \frac{K_B T}{6\pi\eta R_H}$$

where K_B is the Boltzmann constant, T is the temperature, η is the viscosity of the aqueous phase, and R_H is the hydrodynamic radius of a particle, that also equals to the effective diameter (a) obtained from the DLS.

Fluctuations are a result of Brownian motion and can be correlated with the particle diffusion coefficient and size. The correlation function given by the DLS describes the degree of non-randomness in an apparently random signal. Figure 4.1 shows at short delay times, correlation function is high as particles diffuse, as time increases correlation diminishes to zero and the exponential decay of the correlation function is characteristic of the diffusion of the particles. Figure 4.2 shows the correlation function of initial 5 wt% wax-droplets obtained from the dynamic light scattering in a semi-logarithmic plot.

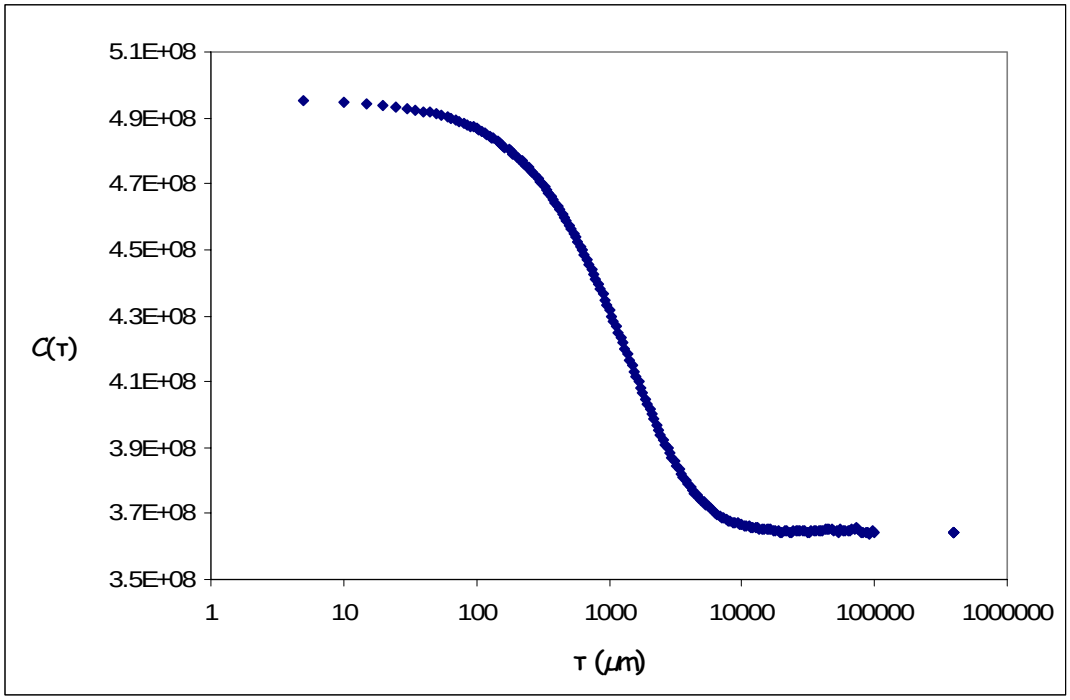

Figure 4.1. Correlation function of initial 5 wt% wax-droplets obtained from the dynamic light scattering.

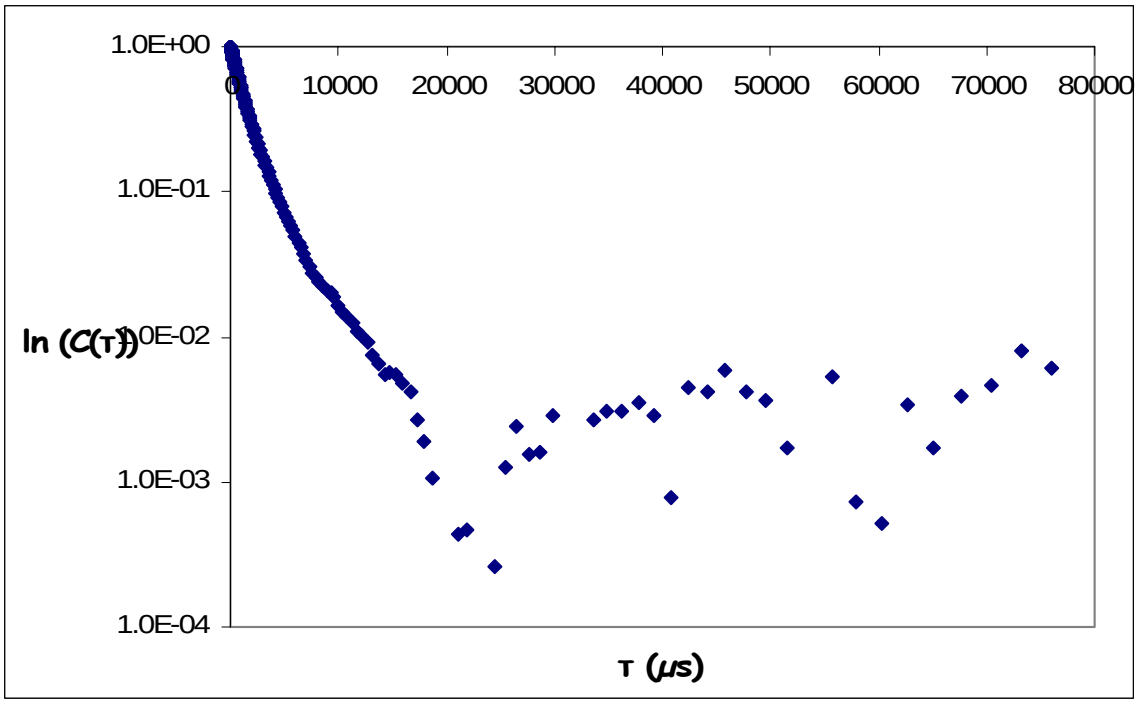

Figure 4.2. Correlation function of initial 5 wt% wax-droplets obtained from the dynamic light scattering in a semi-logarithmic plot.

For a monodisperse samples, single exponential decay will be observed. While for polydisperse samples, a series of exponential decays will be observed instead. Determining the particle size distribution can be done by the analysis of the autocorrelation function with numerically fitting the data with calculations. For our experiment, disk particles sample is analyzed by DLS.

Translational and Rotational Diffusions of Isotropic Wax Particles

The disk-like wax particles produced are certainly not spherical in shape. Therefore, disk particles should not be directly described by the Stokes Einstein equation.

The anisotropic translational coefficient (ε) equation for ellipsoidal particles is described as [21]:

$$\varepsilon = \frac{3}{8}\left[2+\left(\frac{b}{a}\right)^2 - \frac{3\sqrt{\left(\frac{b}{a}\right)^2-1}}{arctg\left[\sqrt{\left(\frac{b}{a}\right)^2-1}\right]}\right]\times\left[\frac{1}{1-\left(\frac{b}{a}\right)^2}\right]$$

for b/a > 1 ellipsoids, where the ellipsoidal particle has the semiaxes a < b = c with axial ratio (b/a). From our experimental data, b/a is about 4, so the anisotropic translational coefficient (ε) is calculated to be -0.446.

The data obtained from DLS gives the effective diameter (a) = 483.5nm, and by rearranging the Stokes Einstein equation:

$$2R_H = 2a = \frac{K_B T}{3\pi\eta D_{eff}} \frac{1}{\sqrt{\left(\frac{b}{a}\right)^2-1}} arctg\sqrt{\left(\frac{b}{a}\right)^2-1}$$

where D_{eff} is the effective diffusion coefficient. By using the aspect ratio (b/a = 4) that we observed from the experimental data, the diameter of disk (b) calculated by DLS is equal to 1.93μm. Compared to the experimental observed diameter of disk which is equal to 1.63μm, the percentage of error is about 15.5%. Possibility of error could be caused by the uncertainty when estimating the size of the disks by using the scale bar from the microscope, as the size of disks are very small that is in the order of micron-meter.

Furthermore, the correlation time for the translational diffusion (τ_T) is obtained from DLS which is equal to 0.0127s. Also, we have estimated the correlation time (τ_R)

for the rotational diffusion and that is obtained by calculating the time between each frame has taken from the video that shows the rotational motion of the disk. Figure 4.3 illustrates a series of pictures have taken for the initial 5 wt%, 2 wt% and 500ppm wax concentrations. The time (t) for the wax disk rotates from its edge into its circular plane has been recorded. Four times this time (4t) is the complete 360 degree rotation of the wax disk particle; and this correlation time (τ_R) for the rotational diffusion is equal to 1.56s.

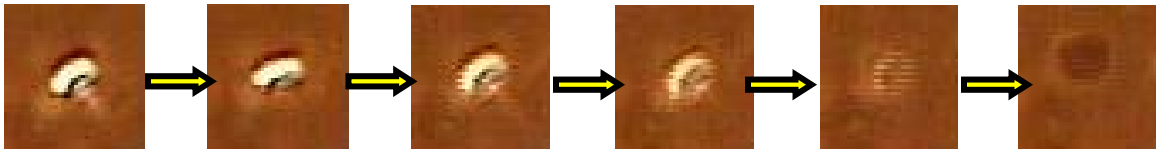

(a)

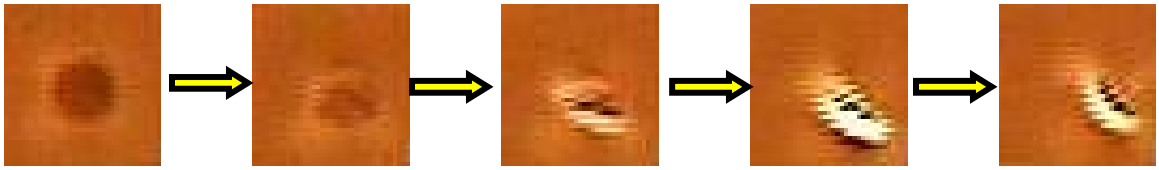

(b)

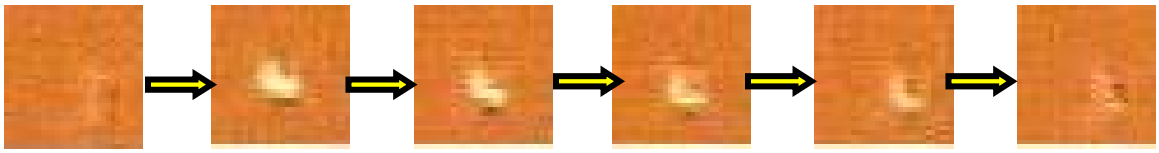

(c)

Figure 4.3. Estimation of the rotational diffusion time (τ_R). It is estimated by calculating the time between each frame from the video that shows the rotational motion of the disk. (a) Initial 5 wt% wax concentration disk-like particle. (b) Initial 2 wt% wax concentration disk-like particle. (c) Initial 500ppm wax concentration disk-like particle.

CHAPTER V

CONCLUSIONS

Microdisks are interested in our research studies because are in great interest of different industries, for example, clay particles in agriculture, asphaltenes in heavy oil industry, and red blood cell in cell biology.

By using our three-dimensional glass microfluidic device, uniform size wax droplets surrounded by 20mM SDS solution are produced. Then surface evaporation of chloroform is performed, so that nucleation and growth of wax particles can occur. The phase transition from isotropic to smectic phase is observed under the polarized light microscope, as the wax particles in anisotropic phase show the birefringence characteristic. As phase transition occur at low temperature, wax droplets changed its spherical shape into disk shape. Also, we observed the diameter, population, and aspect ratio of disks are changing with time. A model of wax particle formation is proposed, and the final number of wax particles split is calculated by using the mass balance equation. Uniform microdisks around 1μm size are produced by emulsion evaporation of the initial 50μm size droplets.

Dynamic light scattering (DLS) is also used to characterize the size of the wax particles. The correlation function obtained from DLS gives us information of the effective diameter for diffusion, polydispersity, translational delay time. For our wax disks, axisymmetric Brownian particles, both translational and rotational diffusions should be considered. Both translational and rotational diffusion coefficients are

calculated by the equations established by Brenner for the axisymmetric Brownian particles. Also, the rotational delay time was estimated by taking frames of pictures from the disk rotation videos that we obtained from the experiment.

REFERENCES

[1] Chandrasekhar, S., and G.S. Ranganath, "Discotic liquid crystals," *Reports on Progress in Physics*, **53**, 57-84 (1990).

[2] Thorne, J.D., and D.J. Pine, "Photonic crystals from emulsion templates," *Advanced Materials*, **13**, 447-450 (2001).

[3] Fernandez, A., G. Cristobal, V. Garces, G.C. Spalding, K. Dholakia, and D.A. Weitz, "Optically anisotropic colloids of controllable shape," *Advanced Materials*, **17**, 680-684 (2005).

[4] Yunus, A.C., *Heat transfer: a practical approach*, 2nd edition, McGraw-Hill Companies, Inc., New York (2003).

[5] Kim, J.Y., J.Y. Baek, K.A. Lee, and S.H. Lee, "Automatic aligning and bonding system of PDMS layer for the fabrication of 3D microfluidic channels," *Sensors and Actuators A: Physical Issue 2*, **119**, 593-598 (2005).

[6] Holden, M.A., S. Kumar, A. Beskok, and P.S. Cremer, "Microfluidic diffusion diluter: bulging of PDMS microchannels under pressure-driven flow," *Journal of Micromechanics and Microengineering*, **13**, 412-418 (2003).

[7] Jeong, W., J. Kim, J. Choo, E.K. Lee, D.J. Beebe, G.H. Seong, and S. Lee, "Continuous fabrication of biocatalyst immobilized microparticles using photopolymerization and immiscible liquids in microfluidic systems," *Langmuir*, **21**, 3738-3741 (2005).

[8] Hu, S., X. Ren, M. Bachman, C.E. Sims, G.P. Li, and N.L. Allbritton, "Surface-directed, graft polymerization within microfluidic channels," *Analytical Chemistry*, **76** (2004).

[9] Whitesides, G.M., and A.D. Stroock, "Flexible methods for microfluidics," *Physics Today*, **54**, 42-48 (2001).

[10] Cheng, Z., P.M. Chaikin, and T.G. Mason, "Light streak tracking of optically trapped thin microdisks," *Physical Review Letters*, **89**, 108303-1-108303-4 (2002).

[11] Brenn, G., "Concentration fields in evaporating droplets," *International Journal of Heat and Mass Transfer*, **48**, 395-402 (2005).

[12] Chang, S.T., and O.D. Velev, "Evaporation-induced particle microseparations inside droplets floating on a chip," *Langmuir*, **22**, 1459-1468 (2006).

[13] Gang, H., O. Gang, H.H. Shao, X.Z. Wu, J. Patel, C.S. Hsu, M. Deutsch, B.M. Ocko, and E.B. Sirota, "Rotator phases and surface crystallization in α-eicosene," *Journal of Physical Chemistry B*, **102**, 2754-2758 (1998).

[14] Leong, K.H., "Morphological control of particles generated from the evaporation of solution droplets: theoretical considerations," *Journal of Aerosol Science*, **18**, 511-524 (1987).

[15] Anderson, V.J., and H.N.W. Lekkerkerker, "Insights into phase transition kinetics from colloid science," *Nature*, **416**, 811-815 (2002).

[16] Conti, M., A. Lipshtat, B. Meerson, "Scaling anomalies in the coarsening dynamics of fractal viscous fingering patterns," *Physical Review E*, **69**, 031406-1-4 (2004).

[17] Buchanan, M., "Liquid crystal foams: formation and coarsening," *Physical Review Letters*, submitted in 2006.

[18] Cheng, Z., A. Fernandez, M. Marquez, D.A. Weitz, T.G. Mason, and P.M. Chaikin, "Manipulation of microdisks in laser tweezers," *The International Society for Optical Engineering*, **5514**, 99-108 (2004).

[19] Davidson, M.W., and M. Abramowitz, "Optical Microscopy" http://micro.magnet.fsu.edu/primer/opticalmicroscopy.html, (1999).

[20] Koysal, O., S.E. San, S. Ozder, and F.N. Ecevit, "Novel approach for the determination of birefringence dispersion in nematic liquid crystals by using the continuous wavelet transform," *Institute of Physics Publishing*, **14**, 790-795 (2003).

[21] Bordi, F., C. Cametti, A.D. Biasio, M. Angeletti, and L. Sparapani, "Quasi-elastic light scattering from large anisotropic particles: application to the red blood cells," *Bioelectrochemistry*, **52**, 213-221 (2000).

VITA

Susanna Wing Man Wong received her Bachelor of Science degree in chemical engineering from the University of California, San Diego in 2004. She entered the chemical engineering Master of Science program at Texas A&M University in August 2004, and she received her Certificate of Business in December 2005 and her Master of Science degree in May 2006.

Ms. Wong may be reached at Department of Chemical Engineering, Texas A&M University, 3122 TAMU, College Station, TX 77843-3122, USA. Her email address is susanna.wong@chemail.tamu.edu.